REPORT DOCUMENTATION PAGE

Form Approved OMB NO. 0704-0188

1. REPORT DATE (DD-MM-YYYY)	2. REPORT TYPE	3. DATES COVERED (From - To)
30-07-2016	Final Report	1-Jun-2012 - 31-May-2016

4. TITLE AND SUBTITLE
Final Report: Experimental Studies of Hydrocarbon Flame Phenomena: Enabling Combustion Control

5a. CONTRACT NUMBER
W911NF-12-1-0140

5b. GRANT NUMBER

5c. PROGRAM ELEMENT NUMBER
611102

6. AUTHORS
Kevin M. Lyons

5d. PROJECT NUMBER

5e. TASK NUMBER

5f. WORK UNIT NUMBER

7. PERFORMING ORGANIZATION NAMES AND ADDRESSES
North Carolina State University
2701 Sullivan Drive
Admin Srvcs III, Box 7514
Raleigh, NC 27695 -7514

8. PERFORMING ORGANIZATION REPORT NUMBER

9. SPONSORING/MONITORING AGENCY NAME(S) AND ADDRESS (ES)
U.S. Army Research Office
P.O. Box 12211
Research Triangle Park, NC 27709-2211

10. SPONSOR/MONITOR'S ACRONYM(S)
ARO

11. SPONSOR/MONITOR'S REPORT NUMBER(S)
61381-EG.23

12. DISTRIBUTION AVAILIBILITY STATEMENT
Approved for Public Release; Distribution Unlimited

13. SUPPLEMENTARY NOTES
The views, opinions and/or findings contained in this report are those of the author(s) and should not contrued as an official Department of the Army position, policy or decision, unless so designated by other documentation.

14. ABSTRACT
This report summarizes the research accomplished in the project "Experimental Studies of Hydrocarbon Flame Phenomena: Enabling Combustion Control". The main areas of activity are: a) electrostatic flame and flow control, b) flame hysteresis in heated coflows, c) flame lifting and splitting in heated jet flows and d) flame dynamics in vitiated and heated coflows. The project supported supplies for the experimental effort, graduate students, summer faculty support and conference and research travel.

15. SUBJECT TERMS
Combustion, Flow Control, Flame Control, hydrocarbon combustion

16. SECURITY CLASSIFICATION OF:			17. LIMITATION OF ABSTRACT	15. NUMBER OF PAGES	19a. NAME OF RESPONSIBLE PERSON
a. REPORT	b. ABSTRACT	c. THIS PAGE			Kevin Lyons
UU	UU	UU	UU		19b. TELEPHONE NUMBER: 919-515-5293

Report Title

Final Report: Experimental Studies of Hydrocarbon Flame Phenomena: Enabling Combustion Control

ABSTRACT

This report summarizes the research accomplished in the project "Experimental Studies of Hydrocarbon Flame Phenomena: Enabling Combustion Control". The main areas of activity are: a) electrostatic flame and flow control, b) flame hysteresis in heated coflows, c) flame lifting and splitting in heated jet flows and d) flame dynamics in vitiated and heated coflows. The project supported supplies for the experimental effort, graduate students, summer faculty support and conference and research travel.

Enter List of papers submitted or published that acknowledge ARO support from the start of the project to the date of this printing. List the papers, including journal references, in the following categories:

(a) Papers published in peer-reviewed journals (N/A for none)

Received	Paper
08/03/2014 13.00	James Kribs, Nancy Moore, Tamir Hasan, Kevin Lyons. Nitrogen-Diluted MethaneFlames in the Near-andFar-Field , Journal of Energy Resources Technology, (12 2013): 0. doi:
08/12/2014 17.00	Andrew R. Hutchins, William A. Reach, James D. Kribs, Kevin M. Lyons. Effects of Electric Fields on Stabilized Lifted Propane Flames, Journal of Energy Resources Technology, (04 2014): 0. doi: 10.1115/1.4027407
08/12/2015 19.00	Sylvain Lamige, Kevin M. Lyons, Cédric Galizzi, Manuel Kühni, Éric Mathieu, Dany Escudié. Lifting and splitting of nonpremixed methane/air flames due to reactant preheating, Combustion Science and Technology, (06 2015): 0. doi: 10.1080/00102202.2015.1059829
TOTAL:	**3**

Number of Papers published in peer-reviewed journals:

(b) Papers published in non-peer-reviewed journals (N/A for none)

Received	Paper
08/03/2014 11.00	Andrew Hutchins, William Reach, James Kribs, Kevin Lyons. Effects of Electric Fields1 on Stabilized Lifted2 Propane Flames , , (06 2014): 0. doi:
08/03/2014 12.00	Kevin Lyons, Sylvain Lamige, Cedric Galizzi, Frederic Andre, Manuel Kuhni, Dany Escudie. Burner lip temperature and stabilization of a non-premixed jet flame, Experimental Thermal and Fluid Science, (06 2014): 45. doi:
TOTAL:	**2**

Number of Papers published in non peer-reviewed journals:

(c) Presentations

Number of Presentations: 0.00

Non Peer-Reviewed Conference Proceeding publications (other than abstracts):

Received	Paper
TOTAL:	

Number of Non Peer-Reviewed Conference Proceeding publications (other than abstracts):

Peer-Reviewed Conference Proceeding publications (other than abstracts):

Received		Paper
07/31/2013	2.00	James Kribs, Andrew Hutchens, William Reach, Tamir Hassan, Kevin Lyons. EFFECTS OF HYDROGEN ENRICHMENT ON THE REATTACHMENT AND HYSTERESIS OF LIFTED METHANE FLAMES, Proceedings of the ASME 2013 Power Conference. 29-JUL-13, . : ,
07/31/2013	9.00	Sylvain Lamige, Cédric Galizzi, Dany Escudié , Frédéric André , Manuel Kühni, Kevin M. Lyons. Influence of heat transfer on jet flame stabilization, European Combustion Meeting (ECM) 2013, Malmo Sweden. 25-JUN-13, . : ,
07/31/2013	8.00	Andrew Hutchens, James Kribs, Richard Muncey and Kevin Lyons. ASSESSMENT OF STABILIZATION MECHANISMS OF CONFINED, TURBULENT, LIFTED JET FLAMES: EFFECTS OF AMBIENT COFLOW, Andrew Hutchens, James Kribs, Richard Muncey and Kevin Lyons. 29-JUL-13, . : ,
07/31/2013	7.00	Andrew Hutchens, James Kribs, Richard Muncey, William Reach and Kevin Lyons. EXPERIMENTAL OBSERVATIONS OF NITROGEN DILUTED ETHYLENE AND METHANE JET FLAMES, ASME 2013 Summer Heat Transfer Conference. 14-JUL-13, . : ,
08/03/2014	16.00	Sylvain Lamige, Cedric Galizzi , Manuel Kühni, Kevin Lyons, Frederic André, Dany Escudié. ON HEAT TRANSFER IN THE STABILIZATION ZONE OF AN ATTACHED METHANE FLAME IN AIR COFLOW, 15th International Heat Transfer Conference, IHTC-15, Kyoto Japan. 08-AUG-14, . : ,
08/03/2014	14.00	Sylvain Lamige, Kevin Lyons, Cedric Galizzi, Frederic Andre, Manuel Kuhni, Dany Escudie. BURNER LIP TEMPERATURE AND STABILIZATION OF A NON-PREMIXED JET FLAME, 8th Mediterranean Combustion Conference. , . : ,

TOTAL: **6**

Number of Peer-Reviewed Conference Proceeding publications (other than abstracts):

(d) Manuscripts

Received		Paper
07/30/2016	18.00	Andrew R. Hutchins, James D. Kribs, Kevin M. Lyons. Effects of Diluents on Lifted Turbulent Methane and Ethylene Jet Flames, ASME Journal of Energy Resouces Technolgy (06 2014)
07/30/2016	1.00	Sylvain Lamige, Jiesheng Min, , Cédric Galizzi, , Frédéric André, , Françoise Baillot, Dany Escudié, , Kevin M Lyons. On preheating and dilution effects in non-premixed jet flame stabilization , Combustion and Flame (07 2012)
07/30/2016	4.00	James Kribs, Nancy Moore, Tamir Hasan, Kevin Lyons. Nitrogen-Diluted Methane Flames in the Near- and Far-Field, Journal of Energy Resources Technology (07 2013)
07/30/2016	5.00	James Kribs, Parth Shah, Andrew Hutchins, William Reach, Richard Muncey, Sean June, Alexei Saveliev, and Kevin Lyons. The Stabilization of Diffusion and Jet Flames in the Presence of High Potential Electric Fields, ASME Journal of Energy Resouces Technolgy (03 2013)
TOTAL:		**4**

Number of Manuscripts:

Books

Received		Book
TOTAL:		

Received	Book Chapter

TOTAL:

Patents Submitted

Patents Awarded

Awards

Graduate Students

NAME	PERCENT_SUPPORTED
FTE Equivalent:	
Total Number:	

Names of Post Doctorates

NAME	PERCENT_SUPPORTED
FTE Equivalent:	
Total Number:	

Names of Faculty Supported

NAME	PERCENT_SUPPORTED	National Academy Member
Kevin M. Lyons	1.00	
FTE Equivalent:	**1.00**	
Total Number:	**1**	

Names of Under Graduate students supported

NAME	PERCENT_SUPPORTED
FTE Equivalent:	
Total Number:	

Student Metrics

This section only applies to graduating undergraduates supported by this agreement in this reporting period

The number of undergraduates funded by this agreement who graduated during this period: 3.00

The number of undergraduates funded by this agreement who graduated during this period with a degree in science, mathematics, engineering, or technology fields:..... 3.00

The number of undergraduates funded by your agreement who graduated during this period and will continue to pursue a graduate or Ph.D. degree in science, mathematics, engineering, or technology fields:..... 2.00

Number of graduating undergraduates who achieved a 3.5 GPA to 4.0 (4.0 max scale):..... 2.00

Number of graduating undergraduates funded by a DoD funded Center of Excellence grant for Education, Research and Engineering:..... 0.00

The number of undergraduates funded by your agreement who graduated during this period and intend to work for the Department of Defense 0.00

The number of undergraduates funded by your agreement who graduated during this period and will receive scholarships or fellowships for further studies in science, mathematics, engineering or technology fields:..... 1.00

Names of Personnel receiving masters degrees

NAME

Total Number:

Names of personnel receiving PHDs

NAME

Total Number:

Names of other research staff

NAME PERCENT_SUPPORTED

FTE Equivalent:
Total Number:

Sub Contractors (DD882)

Inventions (DD882)

Scientific Progress

See Attachment

Technology Transfer

Prepared for the U.S. Army Research Office

Supported by ARO Grant/Contract Number: W911NF1210140

Major Technical Accomplishments Description for the Final Report of

Experimental Studies of Hydrocarbon Flame Phenomena: Enabling Combustion Control

PI: Kevin M. Lyons

North Carolina State University

Table of Contents:

PART A: The Stabilization of Partially-Premixed Jet Flames in the Presence of High Potential Electric Fields

Abstract

Numerous research efforts have focused on flame stabilization and emissions. Based on initial experiments, specific mechanisms resulting from the electric fields were chosen to be investigated, namely the chemical, thermal, and ionization mechanisms. Numerical simulations were performed on premixed propane-ozone-air flames to characterize ozone effects on flame speed resulting from the formation of ozone in high potential electric fields. These results were compared against partially premixed flame experiments to observe the dominant influences within leading edge stabilization within high potential electric fields. It was found that he electromagnetic or ionization influences, serve as the dominant effect on the combustion zone.

Introduction

Lifted jet flame stabilization and emissions control have become key issues to industrial boilers and energy generation. To improve the stability of a lifted jet flame or to decrease emissions, it has been found that the application of high potential electric fields provides some useful results [1, 2, 3]. Previous investigations into pure jet flames have focused on the fluid dynamics and heat transfer influences in jet flame stabilization, as well as the thermochemistry [4, 5]. The lifted jet flame problem provides a unique combustion problem with premixed lean, premixed rich, and non-premixed flames occurring simultaneously at different positions along

the flame, which permits the stabilization of the flame at a downstream location from the jet nozzle. Brown, et al. detailed the stabilization mechanisms of pure jet flames at different locations relative to the issuing nozzle (the near, mid, and far field) [6]. Reustch, et al. investigated the effect of heat release on triple flames, the confluence of a premixed rich, premixed lean, and non-premixed flame, showing that accounting for heat release shows a significant increase in the flame speed [7]. There have been many theories involving the fluid dynamic influences in lifted jet flames, highlighted in Lyons' review of experiments in flame stability [8]. For the purpose of this investigation, the turbulent intensity theory, proposed by Kalghatgi [5], and the large eddy theory, from Broadwell, et al. [9], will be considered due to considerations on fuel-mixing within the experimental setup. The turbulent intensity theory postulates that the flame speed of a lifted jet is augmented by the presence of turbulence, which increases the flame speed from the nominal laminar value, to a higher value, listed as a turbulent flame speed [5]. The large eddy theory describes the recirculation of hot products of combustion into the cooler reactants, by eddy vortices, to increase the temperature of the reactants, therefore increasing the flame speed [9]. For the purposes of this study, a non-premixed flame is a non-jet flame, such as a candle flame stabilized on the flammable limit boundary of the fuel and air, a premixed flame, is fully premixed fuel air mixture, and a partially premixed flame is a jet flame issuing from a central nozzle into air burning with attributes of both premixed and non-premixed flames, as shown in previous studies including those by S.H. Chung [10].

Prior to understanding the high potential electric fields influence on a system as complex as a lifted flame, it is necessary to understand how the electric fields influence neutral fluids. In early discussions on the "ionic or electric wind' was a term used to describe a fluid flow driven only from the difference in electric potentials at two locations, Chattock [2] and Robinson [11].

To produce ionic wind, a high potential combined with a favorable electrode geometry, forms an ionizing plasma region in which local molecules are charged [2]. These particles are then attracted to a secondary electrode, which has an opposite charge [2]. This creates a bulk flow from one electrode to the other, as described by Rickard, et al. [12] and Carleton and Weinberg [13]. The forces of this bulk flow, F, have been shown to be equal to

$$\vec{F} = \vec{E}\, e(n_+ - n_-) \tag{1}$$

where ***E*** is the electric field vector, e is the fundamental charge, and *n* is the number density of positive and negative ions, as denoted by the subscript [13]. The local current density, *j*, can be calculated as

$$\vec{j} = \vec{j}_+ + \vec{j}_- = (K_+ n_+ - K_- n_-)\vec{E}\, e \tag{2}$$

where *K* is the electron mobility [13]. The maximum current density that can be achieved prior to secondary ionization has been shown to be

$$j_{max} = (E_b^{\,2} - E_0^{\,2})\, \varepsilon_0 * \frac{K}{2x} \tag{3}$$

If the potential between the primary and secondary electrode increases beyond a critical value, at the maximum current density, the discharging at the secondary electrode occurs at a rate slower than the charging at the primary electrode. The secondary electrode then assumes a charge, creating a reverse flow. The charging of the secondary electrode will be referred to as "secondary ionization" for this purposes of this study, which can be observed through the formation of corona discharges on the secondary electrode. Beyond the formation of the ionic wind, it has been observed that high potentials in ambient air can produce ozone, changing the constituent particles of air [14]. .

For this study, the impacts of the electric fields on a lifted jet were broken down into three major areas, the thermal, ionic, and chemical mechanisms (resulting from the electric fields), results in changes in flame stabilization. The chemical mechanism results from the changes in chemical kinetics and species present resulting from the high potential electric fields, such as the creation of ozone in ambient air in electric fields or the changes in pollutant emissions discussed above. This mechanism was investigated through premixed flame simulations below on propane-air flames with increasing amounts of ozone addition in the oxidizer. The thermal mechanism, where the electric field provides resistive heat transfer from the current passing through the flame, has been extensively investigated as part of previous jet flame studies, and is highlighted below. The ionic mechanisms, such as the ionic wind and other ionic transport properties, are caused by the electrohydrodynamic forces acting within the flame, in conjunction with the applied electric field. The ionic wind has been observed and documented in previous research, shown in the discussion of the ionic wind later in the study. A graphic illustrating the effects of each mechanism is shown below in Fig. 1.

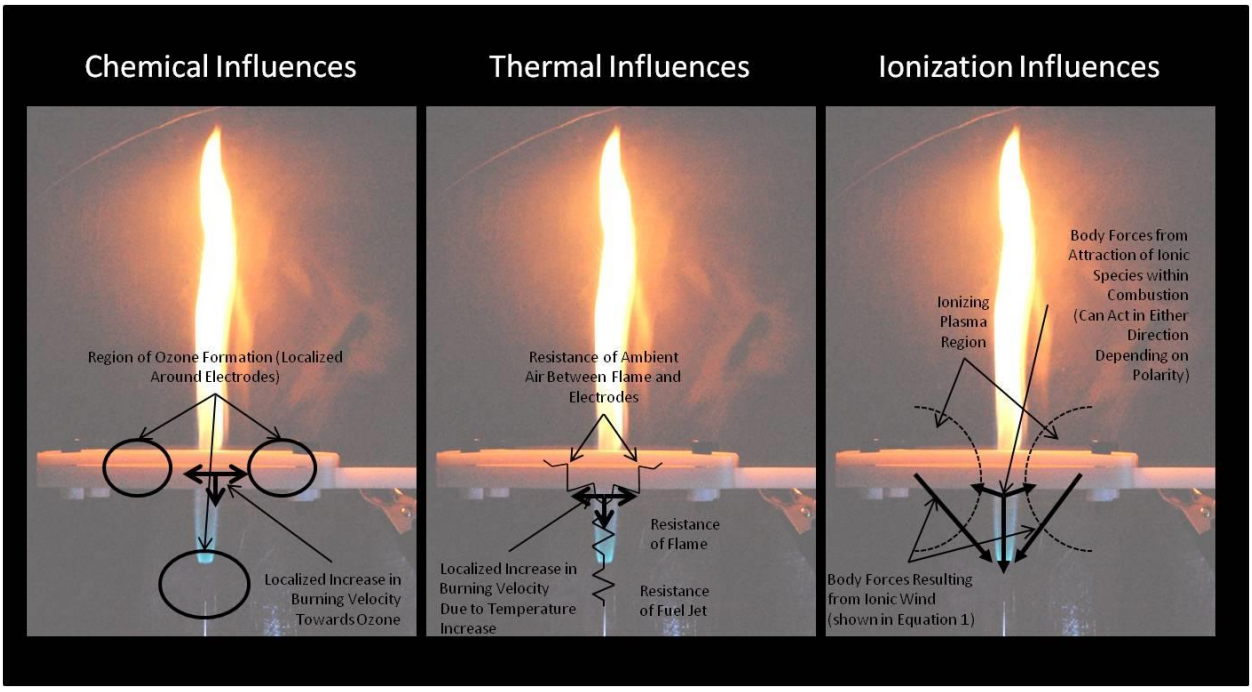

Fig. 1 Comparison of Dominant Influences Resulting from the Application of Electric Fields to Lifted Jet Propane Flames

Experimental Methods

All experiments were conducted in the Reacting Flows and Turbulent Jets Laboratory in the Department of Mechanical and Aerospace Engineering at North Carolina State University, in conjunction with simulations run by the High Pressure and Laser Diagnostics Laboratory.

Experiments on partially premixed flames used propane (CP Grade, 99.0% Pure) issuing from a central nozzle with an inner diameter of 0.8255 mm (.0325 in). The flow rate of the propane was measured through a King 7430 flowmeter and controlled through a MicroLine UHP Gas Panel controller. The primary electrode consisted of a delrin plastic case surrounding a 10

AWG solid core copper wire charging up to 12 needle electrodes on the same loop, though only the one and two needle electrode setup was used in this experiment, as shown in the figure below. The secondary electrode was the nozzle for the issuing jet. The copper wire was inlaid within the electrode case at a diameter of 11.43 cm (4.5 inches) and the internal diameter of the case is 9.60 cm (3.78 inches). The applied voltage was created using an Acopian Positive High Voltage Power Supply (PO30HP2), using voltage control to adjust the power of the electric fields, while allowing the applied current to vary freely. The voltage and current were monitored using dual Agilient Technologies U3401A Multimeters.

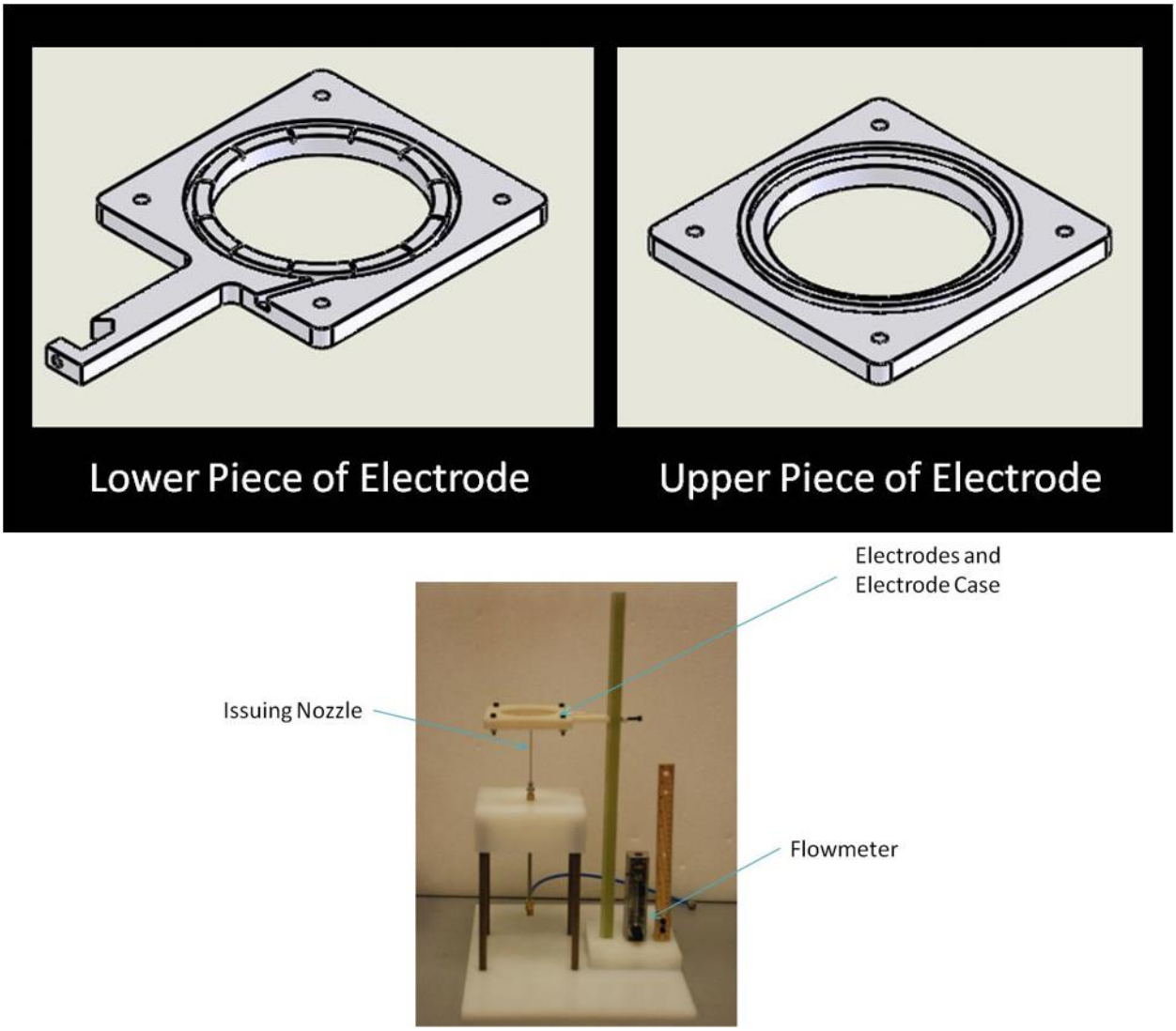

Fig. 2 Experimental Apparatus for Lift Jet Flame Experiments

The electrode polarity of the jet flame experiments was varied, switching between a positively charged primary electrode, and the primary electrode acting as the negatively charged ground. The position of the electrode, relative to the issuing nozzle was held constant at 64.262 mm (2.53 inches) above the nozzle and 23.622 mm (0.93 inches) radially from center of the

nozzle to the tip of the needles. The setup of the burner is shown in Fig. 2. The images of the jet flames were taken using a Nikon D80 digital SLR camera with an 18-135 mm Nikkor Lens, in order to observe the downstream location of the leading edge of the flame, as well as changes in chemiluminescence. The downstream location was determined using Adobe® Photoshop® using the ruler attached to the burner to determine a comparable length scale.

The experimental apparatus above is electrically insulated at the base to prevent accidental grounding, and all experiments were conducted with a shroud placed over the device to isolate the influences of external air flows, while providing access to outside oxidizer, as well as providing protection from electrical arching during the experiment.

Results and Discussion

Diffusion Flame Experiments

Initial observations, made on candle flames using the same power supply from the partially premixed flame, from the experimental apparatus shown were made to prove the effectiveness of high potentials to adjust flame shape, chemiluminescence, and the possibility of flame suppression. Using paraffin candles, the experiments focused on qualitative observations made at observed voltages. During the initial testing, the flame behavior, shown in the figure below, was observed.

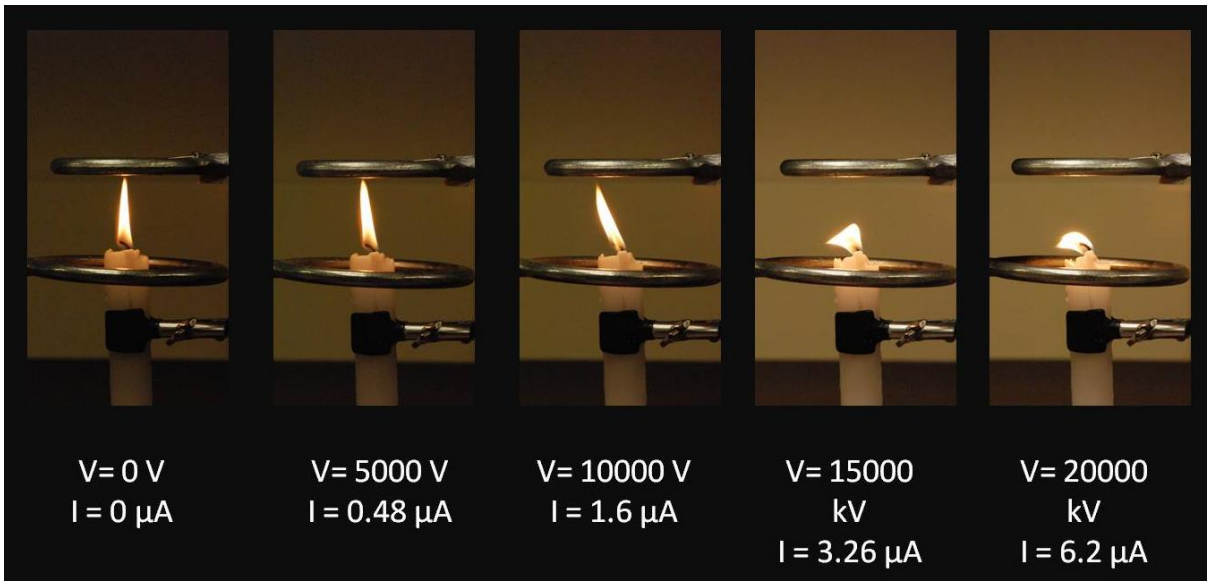

Fig. 3 Comparison of Flame Behavior of Attached Diffusion as a Function of Applied High Voltage

In this single needle electrode configuration, it was observed that the flame was repelled by the presence of the high potential. This effect became more pronounced at higher voltages. The experiment was limited to 20,000 V, as the air surrounding the electrodes would begin to carry a charge and cease acting as a dielectric, creating sparks, which would travel between the clamp for the candle and the grounded ring. While the candle flame responded in a similar way as though there were a counterflowing air acting on the system, the intermittent flickering that would be expected from a diffusion flame in a flow of air was not present, but rather the flame maintained a consistent shape at each applied voltage.

Further observation of the results of the candle flame experiment has shown that not only is the flame shape influenced by the electric field, but also, the products of combustion, specifically soot accumulation. Fig. 4 is a still image taken after the experiment was concluded.

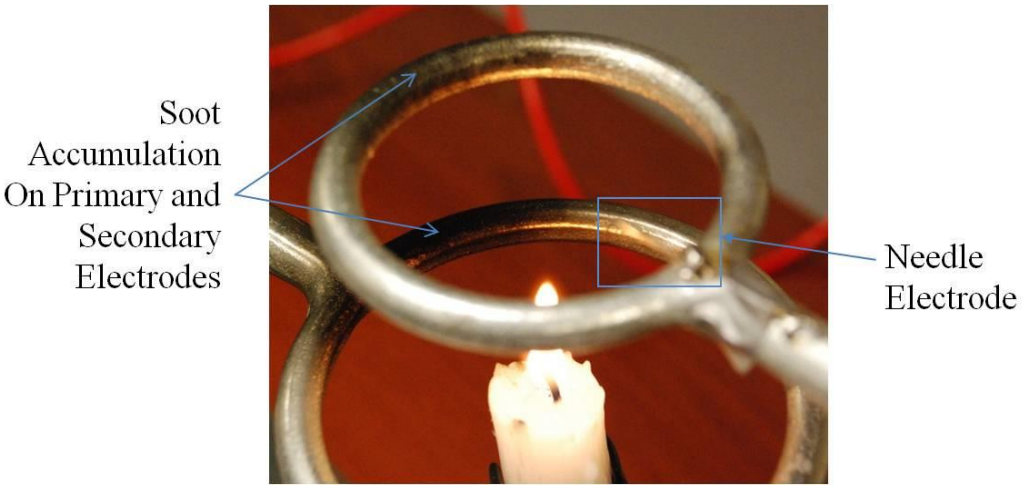

Fig. 4 Attraction of Soot Resulting from Applied Electric Field

As shown in Fig. 4, there is a pronounced buildup of soot on the grounded electrode, away from the needle. This effect has been observed in other experiments, specifically the repulsion of soot by positive electrodes, or attraction of soot by negative electrodes. In the case below, using a negatively charged power supply, the soot and flame would appear on the electrode, with the effect becoming more pronounced as the electrode approached the diffusion flame.

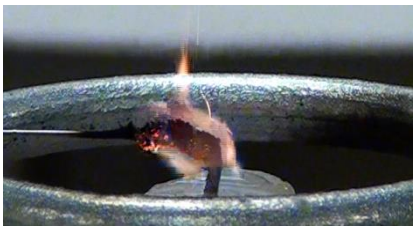

Fig. 5 Soot Attracted to Negatively Charged Electrodes for Small-Scale Candle Flame Experiments

These experiments brought up serious questions into which mechanism of flame manipulation using electric fields dominates and controls the stabilization of the flame. The

main observations on the attraction of soot and the flame shape manipulation, similar to counterflowing air experiments, brought into question whether certain influences were more significant than other forces. By applying an outside electric field, there are three major factors that must be accounted for, specifically the thermal effects resulting from the resistive heating within the flame, the introduction of new chemical species to the reactants, such as ozone formation from corona discharges, and the ionization effects, such as the ionic wind and the attraction and repulsion of charged species. The thermal effects, specifically the influence of increased temperature on factors, such as flame speed have been well documented in past tests [37, 38], and the ionic influences have been reviewed above, while the influence of chemical species expected results need to be compared to a partially premixed flame under an electric field. For this reason, a premixed flame simulation was run with the addition of ozone to the oxidizer stream, in order to compare the influence of ozone creation to the experimental observations on the partially premixed flame.

Premixed Flame Simulations

Fully premixed flames provide useful insight into the basic mechanisms in flame liftoff, allowing for the calculations of laminar flame speeds. In order to investigate the influence of high potential electric fields resulting from corona discharges on premixed flames, a specific mechanism, the formation of ozone issuing from the corona was investigated. The formation of ozone was chosen as it is one of the major changes to the reactants resulting from an electric field. Previous studies into the effects of ozone addition to a flame have been conducted [14],

but a wider range of ozone concentration was chosen for this study, in order to completely understand the impacts. In the investigation by Ombrello et al. [14], it was found that the addition of ozone did improve flame front stabilization with experiments adding ozone to a coflowing air, as well as numerical simulations. These simulations provided a necessary baseline for comparison, within the partially premixed experiments conducted later, on the effect of the ozone addition, and expected flame behavior. The simulations show how does ozone addition influence the stabilization of the leading edge of the flame, in the form of changes in laminar flame speed, and what changes in chemiluminescence would result from the addition of ozone, as these effects are not well documented.

The PREMIX package within chemical kinetic package, Cantera, was used to determine the OH concentration, as well as the laminar flame speed, S_L, for increasing concentrations of ozone addition in the oxidizer, from the flame front to a position 0.1m downstream. The amount of O_3 was varied from 0 ppm to 10,000 ppm. The concentrations of OH for 3 concentrations of ozone (0, 5000, 10000 ppm) are shown below, in Fig. 6.

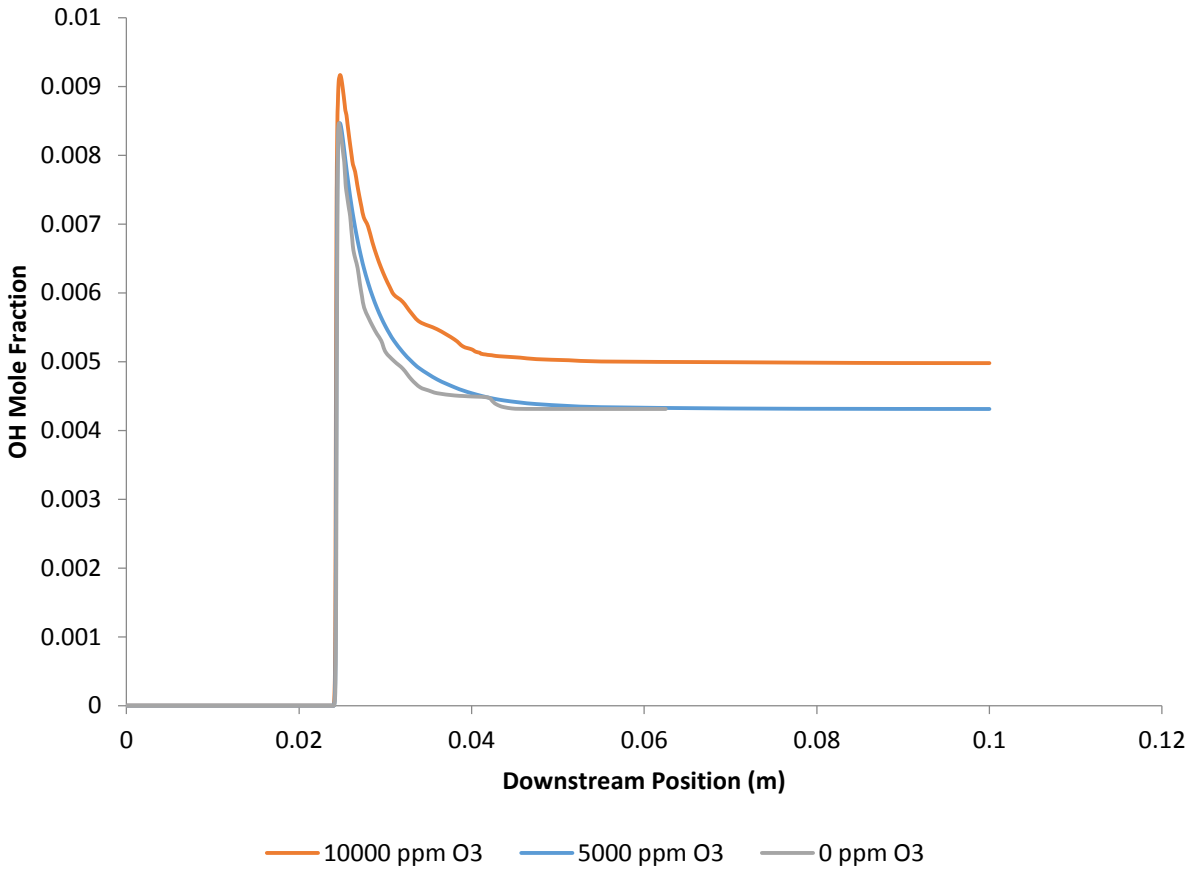

Fig. 6 OH Mole Fraction for Premixed Flame Simulations

The OH mole fraction peak value for the highest concentration of ozone (O_3=10000 ppm) was found to be approximately 20% more than for the standard case (O_3=0 ppm). Further investigation, showing a comparison of the change in OH concentration resulting from ozone addition, as well as the change in laminar flame speed, is shown below in Fig. 7.

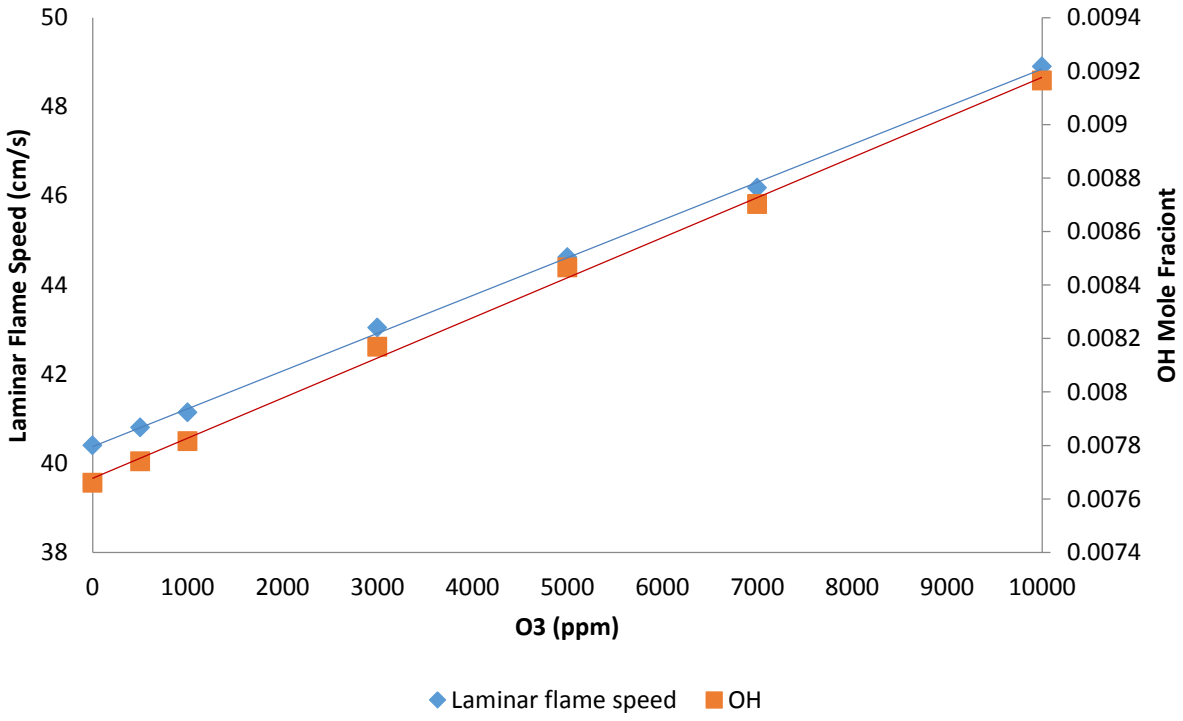

Fig. 7 Laminar Flame Speed and Peak OH Mole Fraction as a Function of O3 Concentration in the Reactants of a Premixed C3H8 Flame

Based on these observations, it would be expected that as the amount of applied voltage increases, thereby increasing the amount of ozone formation from the resulting corona discharge, the laminar flame speed of a propane flame would increase, as well as the peak amount of OH production, an increase of approximately 20% for both the OH production and laminar flame speed when compared to the standard case. The increase in OH production, shown by OH chemiluminescence, would act as an indicator of the chemical mechanisms, specifically the O_3 production, resulting from the influence of electric fields, was the dominant mechanism affecting the stabilization mechanisms of a lifted jet flame.

It has been shown in previous research that it is possible to adjust the lifted position of partially premixed flame, to another stabilized position upstream or downstream (axially) from the jet stabilized position through the application of electric fields [15, 16]. This localized enhancement or suppression of the flame front was investigated in positive and negative polarity configurations (referring to the polarity of the primary electrode, the ring), in a single and double needle setup, over 6 flow rates between 1.14 to 1.53 liters per minute (2.4-3.2 scfh). An example of the resulting flame is shown in the figure below.

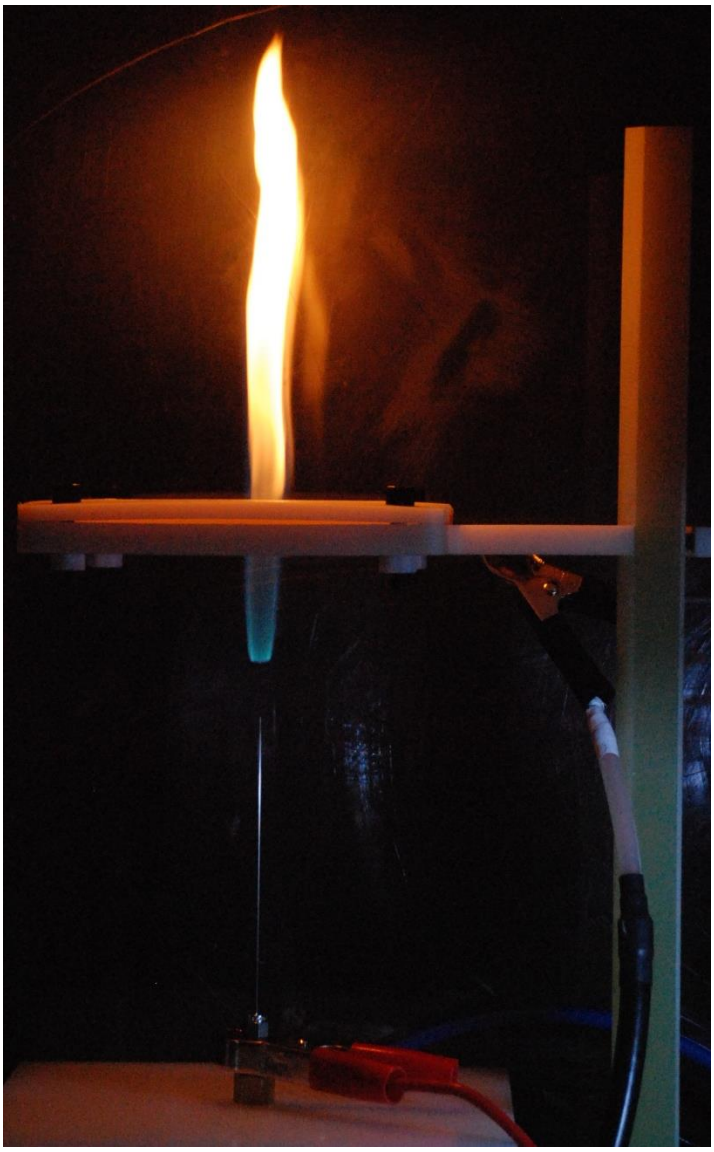

Fig. 8 Sample Stabilized, Partially Premixed Jet Flame at 1.14 slpm and 4000 V (Liftoff Height=1.78 cm)

The voltage applied to create the electric field was varied until either the flame reattached, which was found to be the result for the positive configurations, or blowout, for the negative configurations, respectively. The flow rates were fixed between tests, and the voltage varied to witness the effect on the flame, with photos taken of the leading edge of the flame at approximately 1000V increments. The different configurations and applied voltages are shown

below in Table 1, and a demonstration of the positive versus negative electrode configuration is shown in the figure below.

Table 1- Electrode Configurations and Applied Voltages for Partially Premixed Flame Experiments

Primary Electrode Polarity	**Number of Primary Electrodes**	**Applied Voltage**
Negative	1	0-12,000 V
Negative	2	0-12,000 V
Positive	1	0-5,000 V
Positive	2	0-5,000 V

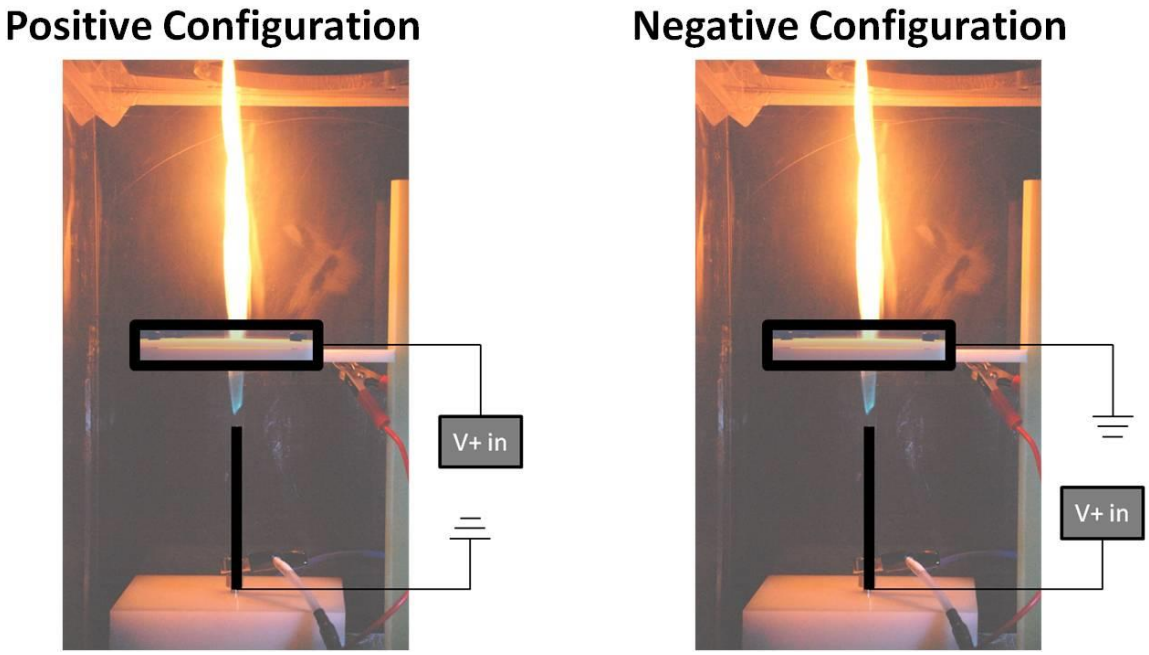

Fig. 9 Layout of Positive and Negative Configurations for the Lifted Jet Flame Experiments

The average lifted position of the flame was plotted against the applied voltage, shown in figures 5a-f.

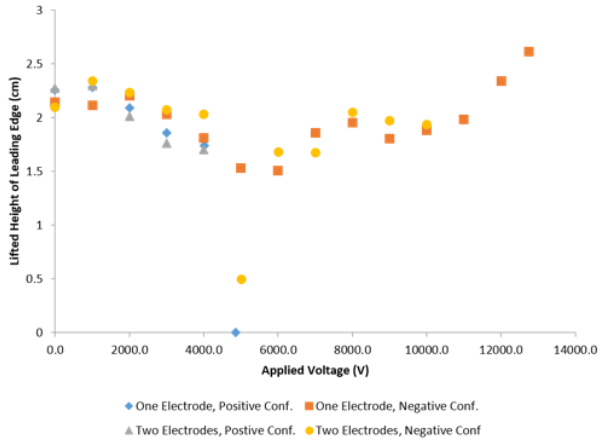
Lifted Height of Leading Edge (cm)
Applied Voltage (V)
One Electrode, Positive Conf.
One Electrode, Negative Conf.
Two Electrodes, Postive Conf.
Two Electrodes, Negative Conf

A

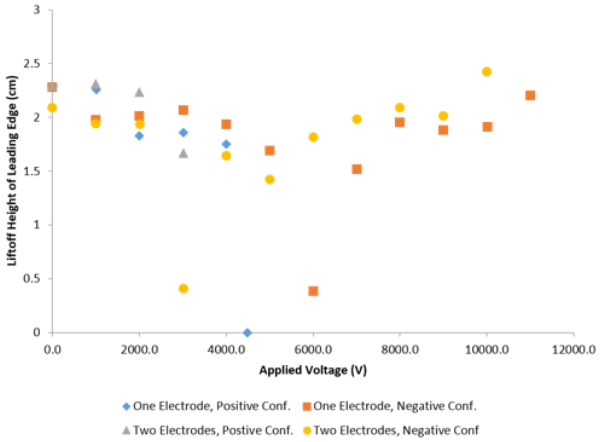
Liftoff Height of Leading Edge (cm)
Applied Voltage (V)
One Electrode, Positive Conf.
One Electrode, Negative Conf.
Two Electrodes, Postive Conf.
Two Electrodes, Negative Conf

B

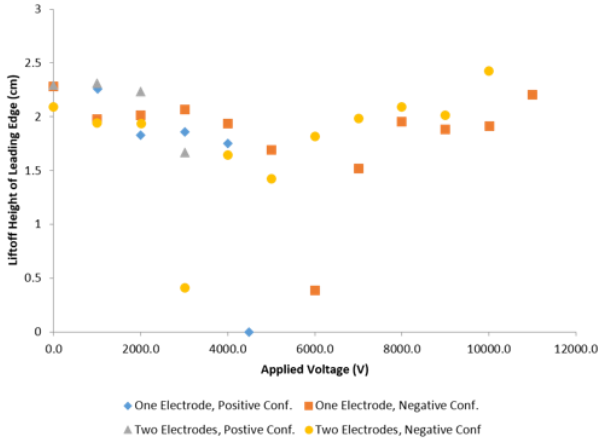
Liftoff Height of Leading Edge (cm)
Applied Voltage (V)
One Electrode, Positive Conf.
One Electrode, Negative Conf.
Two Electrodes, Postive Conf.
Two Electrodes, Negative Conf

C


Liftoff Height of Leading Edge (cm)
Applied Voltage (V)
One Electrode, Positive Conf.
One Electrode, Negative Conf.
Two Electrodes, Postive Conf.
Two Electrodes, Negative Conf

D

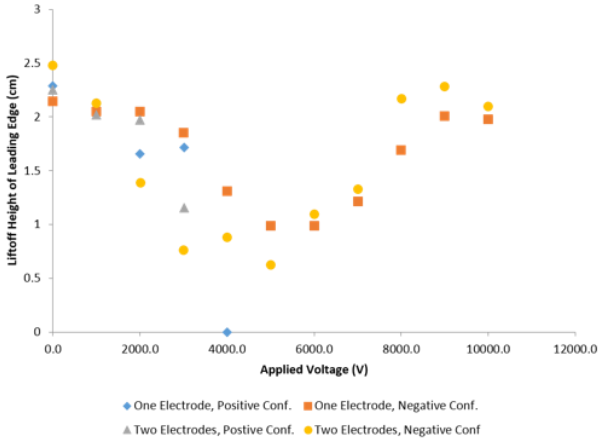
Liftoff Height of Leading Edge (cm)
Applied Voltage (V)
One Electrode, Positive Conf.
One Electrode, Negative Conf.
Two Electrodes, Postive Conf.
Two Electrodes, Negative Conf

E

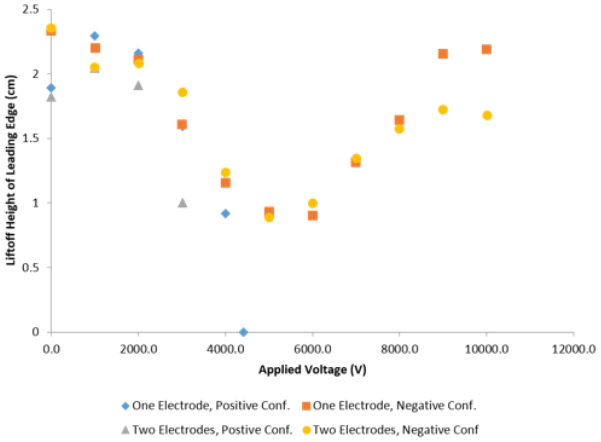
Liftoff Height of Leading Edge (cm)
Applied Voltage (V)
One Electrode, Positive Conf.
One Electrode, Negative Conf.
Two Electrodes, Postive Conf.
Two Electrodes, Negative Conf

F

Figure 10a-f- Location of the Leading Edge of the Flame for Applied Voltage (1.14 SLPM through 1.53 SLPM)

Figures 6a through f provide useful insight into the electric field effects within lifted flames. The overall trends with the same electrode configuration (positive or negative polarity) remained similar for each flow rate. The positive configurations, for both one and two electrode setups, saw a decrease in liftoff height until the flame reattached at approximately 4 kV, and remained attached at higher voltages. The reattachment for the positive configuration occurred at the same voltage, independent of the number of electrodes, and while the trends for the two electrode setups were not the same, where it was observed that the two electrode setup was more effective for most flow rates, there was no definitive advantage to using multiple electrodes.

The negative configurations saw a marked decrease in liftoff height following trends similar to the positive configurations, at low voltages (below 6 kV), where the flame would intermittently attach and liftoff after 3 kV, at approximately 4.5 kV, then the leading edge shifted downstream, eventually blowing out at voltages above 10 kV. Much like the positive configuration, there was no marked difference between utilizing double electrode configuration, with both setups reattaching and then progressing to blowout in the same trends, with the applied voltage at blowout being approximately the same between the setups. The overall observations on the flame stability are shown in the figure below.

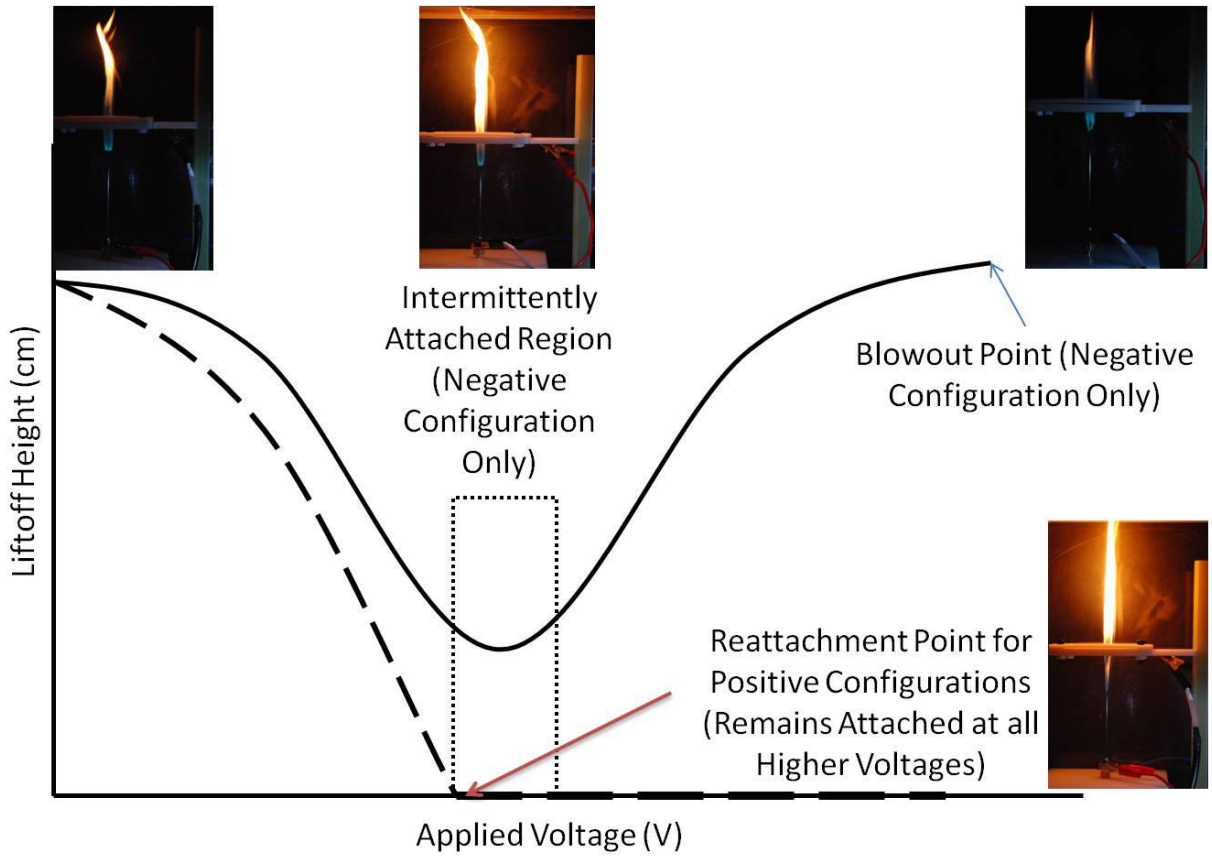

Fig. 11 Characterization of Flame Stabilization Points for Partially Premixed Flames as a Function of Applied Voltage. Negative Configurations are Shown as the Solid Curve, and Positive Configurations are Shown as the Dashed Curve.

The overall trend for the negative configuration could have been a result of secondary ionization at the electrodes, where the maximum charge density, listed in Equation 3, was reached. This would be in agreement with previous studies, on neutral fluids, such as June, et al. [17], where the influences of the ionic wind decreased as the electric field became too strong. The resulting corona discharge seen in June, et al. was not observed [17], but it could have been masked by the chemiluminescence of the flame. Secondary ionization would have occurred at a

lower applied voltage than in previous studies into air flows [18, 17], as the number density of ions, n, would have been higher due to the number of ions produced in combustion.

Further observations into the influence of the current in the applied electric field provided little insight into the stabilization mechanisms. Using the experimental setup, with the current floating, resulted in a near constant current at approximately 0.013-0.016 mA for both configurations at voltages below 3,000 V. At voltages above 4,000 V, where the positive and negative configurations reattach, the current increased by an order of magnitude. While any further adjustment in the positive configuration has no influence, as the flame remained attached, adjusting the voltage, for the negative configuration causes the flame to liftoff further downstream, and the current increases to approximately 0.5 mA at blowout. Plotting the current against the liftoff height resulted in no discernible trends.

The major observation, the difference between the positive and negative configuration trends, provides unique insights into the major influences of electric fields in lifted flames and on the leading edge of the flame. The fact that changing the polarity of the primary electrode downstream has a distinct effect, going as far as causing the flame to blowout in one configuration and reattach in another, shows that the dominant mechanisms in flame stabilization in electric fields. The expected results were compared to observed flame behavior to study the overall dominant mechanisms. For the thermal mechanism, stating that the applied electric field provides resistive heating within the flame, increasing the flame temperature, resulting in an increase in flame velocity, or the speed at which the leading edge of the flame propagates into the incoming stream of the fuel jet. If this were the dominant mechanism, the trends between the two polarities would have been the same, as resistive heating would provide the same amount of

heat and therefore, the same increase in flame temperature, regardless of polarity. Specifically, the blowout, observed in the negative configurations, would not have been observed.

The main chemical mechanism considered in this study, the formation of ozone (O_3) resulting from the presence of high voltages, as shown in the numerical simulations, would have seen a marked increase in flame speed, as shown in the premixed numerical study above. Any increase in ozone formation would see the same increase in flame speed, but during an initial testing phase of the experiment, the ionization at the primary electrode caused a local extinction within the flame, shown in the figure below, at 1.30 slpm, contrary to the expected result, as shown in the numerical simulations, based on the work in Ombrello, et al. [14], where the flame should see an increase in the flame speed at the electrode.

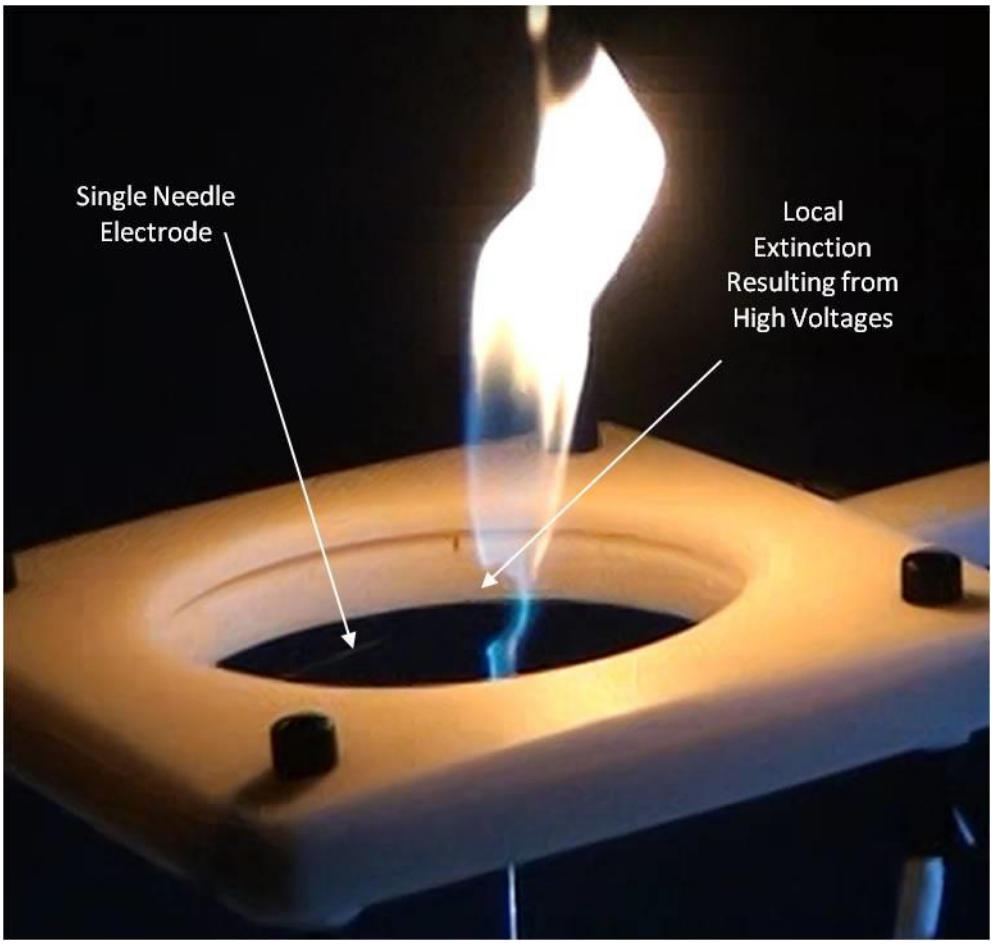

Fig. 12 Local Extinction Resulting from High Potential Electric Fields at Approximately 6950 V with the Negative Polarity, Single Electrode Configuration at 1.30 splm

If the ozone formation were dominant in the stabilization mechanisms, it would be expected to see a localized enhancement of the flame with an increase in flame speed around the electrodes. It would also be expected that the flame would exhibit an increase in OH chemiluminescence, as from the numerical simulation, the ozone addition would cause an increase in the OH formation within the flame. The increase in OH chemiluminescence was not observed in Kim, et al. [19] in experiments using OH-PLIF on laminar flames in electric fields.

For these reasons, the ozone formation, and the chemical mechanisms resulting from the electric field application would not result in the decrease in liftoff height.

This extinction around the electrode provided evidence that the electromagnetic influences dominate the stabilization mechanisms of the leading edge of the flame. The influences of the ionic wind, especially with regards to an already ionized system, such as a partially premixed flame, were found to be the dominant flame control mechanism. The attraction or repulsion of chemical species, such as soot particles, would have had a direct influence on the chemical kinetics of the flame, as it would change the concentration of radicals within the flame front. Combining this influence with the ionic wind body forces, shown in equation 1, which would have acted on the surrounding oxidizer, would explain the reattachment, even the intermittent reattachment and blowout observed for the negative configurations. Blowout could have been a result of the secondary ionization, due to the reaching of the maximum possible charge density, shown in Equation 3, for resulting in a negation of the ionic wind body forces, as well as, increased attraction and repulsion forces on the existing ions within the flame.

Also of note, the flame structure observed at higher voltages, as shown in the Fig. 13 below at 11,000 V at 1.30 slpm for the single electrode, negative configuration, showed abnormal flow structure with intermittent flames, showing decreased chemiluminescence, but with the signature luminosity of a trailing diffusion flame. Previous studies have indicated that as flames approach blowout, resulting from the increases in central nozzle velocity, the trailing diffusion flame disappearing as an indicator of blowout [20]. The presence of the diffusion flame, while not in the typical manner, indicates that the flame structure itself was not

approaching the flammable limits of the flame, but implies that blowout was a result of the external influence of the electric field.

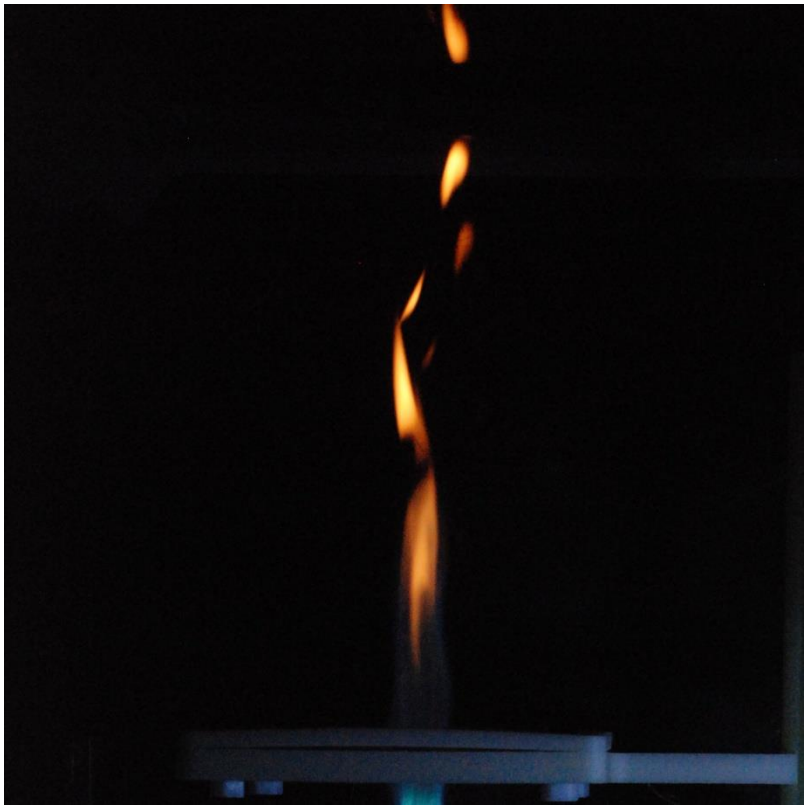

Fig. 13 Abnormal Flame Structure of the Trailing Diffusion Flame at 11000 V at 1.30 slpm

4. Conclusions

Previous experiments on the impacts of high potential electric fields on combustion have shown the ability to manipulate the liftoff height of jet flames, remove pollutants, and alter flame structure and hence, chemiluminescence. The purpose of this study was to observe the dominant mechanisms within leading edge stabilization in the applications of electric fields in partially premixed, jet flames, comparing the influence of thermal, chemical, and ionic impacts. Numerical simulations of premixed propane flames with ozone formation resulting from a

corona discharge showed an increase in OH formation, as well as laminar flame speed, with increasing ozone concentration in the reactants, in order to observe the expected influences of chemical mechanisms within the partially premixed flame. Further investigation into partially premixed, propane jet flames, showed:

a) With a positively charged electrode downstream of the leading edge of the flame, it was possible to reattach a lifted jet flame, while maintaining a constant fuel flow rate.
b) With a negatively charged electrode downstream of the leading edge, the liftoff height was shortened at voltages below 4000 V, after which the leading edge shifted downstream of the nozzle, and reached blowout at approximately 10000 V.
c) The ionizing influence of the applied electric field is the dominant influence of the high potentials, rather than thermal influences or changes to the chemical kinetics of the combustion event.
d) Blowout, in the negative configuration, did not show the expected markers of reaching the flammability limits of the fuel-air mixture, with the trailing diffusion flame remaining until blowout.

These conclusions show that jet flame behavior, with regard to the stabilization point of the flame at a set fuel velocity, was absent at high potentials, with regards to liftoff, reattachment, and blowout, which have been extensively investigated in the past. Further study is necessary in the concentrations, and flow directions, of ionic species within flames under electric fields.

Works Cited

[1] W. Brade, "The Bakerian Lecture: on some new Electro-chemical Phenomena," *Philosophical Transactions of the Royal Society of London,* vol. 104, pp. 51-61, 1814.

[2] A. Chattock, "On the Velocity and Mass of Ions in the Electric Wind in Air," *The London, Edinburgh and Dublin Philosophical Magazine and Journal of Science,* vol. 48, no. 294, pp. 401-420, 1899.

[3] R. J. Bowser and F. J. Weinberg, "Electrons and the Emission of Soot in Flames," vol. 249, 1974.

[4] S. Chung, "Stabilization, propagation and instability of tribrachial triple flames," *Proceedings of the Combustion Institute,* pp. 877-892, 2007.

[5] G. Kalghatgi, "Lift-Off heights and visible lengths of vertical turbulent jet diffusion flames in still air," *Combustion Science and Technology,* vol. 41, no. 1-2, pp. 17-29, 1984.

[6] C. Brown, K. Watson and K. Lyons, "Studies of lifted jet flames: stabilization in the near- and far-fields," *Flows, Turbulence and Combustion,* pp. 249-73, 1999.

[7] G. Ruetsch, L. Vervisch and L. Williams, "Effects of heat release in triple flames," *Physics of Fluids,* vol. 7, no. 6, pp. 1447-54, 1995.

[8] K. Lyons, " Toward an understanding of the stabilization mechanisms of lifted turbulent jet flames: experiments," *Progress in Energy and Combustion Science,* pp. 211-31, 2007.

[9] J. Broadwell, W. Dahm and M. Mungal, "Blowout of Turbulent Diffusion Flames," *Proceedings of the Combustion Institute,* vol. 20, no. 1, pp. 303-310, 1984.

[10] B. Lee and S. Chung, "Stabilization of lifted Tribrachial flames in a laminar nonpremixed jet," *Combustion and Flame,* vol. 109, pp. 163-72, 1997.

[11] M. Robinson, "A History of the Electric Wind," *American Journal of Physics,* vol. 30, no. 5, pp. 366-72, 1962.

[12] M. Rickard, D. Dunn-Rankin, F. Weinberg and F. Carleton, "Maximizing ion-driven gas flows," *Journal of Electrostatics,* vol. 64, no. 6, pp. 368-376, 2006.

[13] F. Carleton and F. Weinberg, "Electric field-induced flame convection in the absence of gravity," *Nature,* vol. 330, pp. 635 - 636, 1987.

[14] T. Ombrello, S. Won, Y. Ju and S. Williams, "Flame propagation enhancement by plasma excitation of oxygen. Part I: Effects of O3," *Combustion and Flame,* vol. 157, pp. 1906-

1915, 2010.

[15] G. Pilla, D. Galley, D. A. Lacoste, F. Lacas, D. Veynante and C. O. Laux, "Stabilization of a Turbulent Premixed Flame Using a Nanosecond Repetitively Pulsed Plasma," *IEEE Transactions on Plasma Science,* vol. 34, no. 6, pp. 2471-77, December 2006.

[16] K. Criner, A. Cessou and P. Vervisch, "A Comparative Study of the Stabilization of Propane Lifted Jet-Flames by Pulsed, AC and DC High-Voltage Discharges," in *Proceedings of the European Combustion Meeting*, 2007.

[17] M. June, J. Kribs and K. Lyons, "Measuring efficiency of positive and negative ionic wind devices for comparison to fans and blowers," *Journal of Electrostatics,* vol. 69, no. 4, p. 345–350, 2011.

[18] J. Kribs, M. June and K. Lyons, "The Effects of Collector Surface Area with Electrostatic Flows Resulting from Multiple Corona Discharges," in *IEEE Pulsed Power Conference*, Washington D.C., 2009.

[19] M. Kim, S. Ryu, S. Won and S. Chung, "Electric fields effect on liftoff and blowoff of nonpremixed laminar jet flames in a coflow," *Combustion and Flame,* vol. 157, pp. 17-24, 2010.

[20] N. Moore, J. McCraw and K. Lyons, "Observations of Jet-Flame Blowout," *International Journal of Reacting Systems,* vol. 2008, pp. 1-8, 2008.

PART B: EFFECTS OF DILUENTS ON LIFTED TURBULENT METHANE AND ETHYLENE JET FLAMES

ABSTRACT

The effects of diluents on the liftoff of turbulent, partially premixed methane (CH_4) and ethylene (C_2H_4) jet flames for potential impact in industrial burner operation for multi-fuel operation have been investigated. Both fuel jets were diluted with nitrogen and argon in separate experiments, and the flame liftoff heights were compared for a variety of flow conditions. Methane flames have been shown to liftoff at lower jet velocities and reach blowout conditions much more rapidly than ethylene flames. Diluting ethylene and methane jets with nitrogen and argon, independently, resulted in varying trends for each fuel. At low dilution levels (~5% by mole fraction), methane flames were lifted to similar heights, regardless of the diluent type; however, at higher dilution levels (~10% by mole fraction) the argon diluent produced a flame which stabilized farther downstream. Ethylene jet flames proved to vary less in liftoff heights with respect to diluent type. Significant soot reduction with dilution is witnessed for both ethylene and methane flames, in that flame luminosity alteration occurs at the flame base at increasing levels of argon and nitrogen dilution. The increasing dilution levels also decreased the liftoff velocity of the fuel, as well as decrease the radial position of the flame. Analysis showed little variance among liftoff heights in ethylene flames for the various inert diluents, while methane flames proved to be more sensitive to diluent type. This sensitivity is attributed to the more narrow limits of flammability of methane in comparison to ethylene, as well as the much higher flame speed of ethylene flames.

Key Words: Turbulent Jet Flames; Flame Liftoff; Blowout; Inert Gas Dilution; Luminosity

1. INTRODUCTION

The investigation of lifted turbulent jet flames is of specific interest for many industrial and commercial applications due to their utilization in furnaces, burners, and boilers. Of particular interest to many industries and branches of the military, in particular the United States Army, is continued improvement in multi-fuel burners. These devices allow for burner operation with various fuels that have different heating values, laminar flame speeds, Schmidt Numbers, etc. Understanding how various flames behave in the near-nozzle region under the various flow conditions can permit the design of clean, stable, durable and efficient combustion systems. Studies on turbulent lifted flames have observed the fluctuations of the liftoff heights, variations of blowout limits, and hysteresis patterns [1-4], and have been reviewed by Pitts [5] and Lyons [6]. It is well known that turbulent jet flames liftoff from the fuel supply nozzle as the velocity of the fuel is increased beyond a critical point. As the flame experiences the transition from attached to the nozzle to lifted, the luminosity of the flame is altered due to local air-fuel mixing and temperature variations.

Wilson and Lyons [7] investigated the effect of diluents on methane and ethylene flame temperatures and burning velocities and found that the addition of these diluents have significant influences on flame behavior. For nitrogen dilution, Wilson [7] found that increasing amounts of nitrogen additive lowered the laminar burning velocity and flame temperature. As a follow-up on this work [7], Wilson suggests that studies investigate other trends that might be present when observing fuel/diluent combinations, in particular at the leading edge of the flame. Stamps and Tieszen [8] used the Kalghatgi model in [20] to compare the blowout limits of diluted hydrogen and ethylene flames. The predictions modified in this paper, however, use the Broadwell scaling

mechanism to scale normalized, diluted methane and ethylene flames. Thus, a main focus of this paper will be how flames diluted with different additives will be affected at the leading edge, as well as leading edge movement from the fuel nozzle.

As the flame jet velocity is increased, the flame will leave the nozzle and stabilize at a certain height that is dependent on fuel velocity and other exterior parameters, such as non-reactive gas addition, coflowing (that is gas, most frequently air, flowing in parallel with jet velocity) annulus parameters [9-10], and flame confinement [11]. This lifted flame will oscillate at a mean lifted height until changes in local stoichiometry, jet velocities, coflow velocities, or combinations of these, alter the stabilization location [12]. Increases in any of the aforementioned parameters will lead to flame blowout shortly after the trailing diffusion flame vanishes [13]. Figure 1 gives a theoretical representation of how the flame progresses with velocity increases. The arrows designate an increase or decrease in fuel velocity and the trend that the flame lift height follows. The arrow designating a decrease in fuel velocity and a liftoff height present at lower fuel velocities than the original propagation represents the hysteresis regime as described by Terry and Lyons [2]. A flame, however, can experience diverse phenomena in which the flame is extinguished directly after leaving the fuel supply nozzle [14-15]. This is known as flame blow off, which occurs when the flame cannot stabilize after lifting off from the nozzle and is immediately extinguished due to fuel velocities that do not permit stabilization of the flame in the given mixture fraction field.

It has been experimentally and theoretically shown that the addition of inert gases to the fuel stream leads to a less stable turbulent diffusion flame [16-21]. Common diluents, such as nitrogen and carbon dioxide, have been well investigated and have proven to have significant effects on the liftoff behavior, as well as blowout limits, of methane jet flames [21]. Gollahalli

[22] found that diluting propane flames with carbon dioxide or nitrogen decreases the flame length and stability. In addition, complete soot suppression was found to be possible with high percentages of diluent addition. Most of these studies involve only the analysis of methane gas with additives, while few investigate the comparison of adding non-reactive gases to higher-order hydrocarbon fuels, such as ethylene [23]. The current experimental study investigates the effect of diluting methane and ethylene jet flames with nitrogen and argon, independently. Phenomena investigated are the lifted flame stability between the two fuels, the flame blowout regime, and the inert diluent additive effects on flame luminosity, in particular, at the flame's leading edge. In addition, a non-dimensional analysis has been performed to determine how previous studies correlate with the measured data. This involved the investigation of a non-dimensional flame liftoff prediction that compares various diluent levels, as well as both fuels, for progressively increasing jet velocities. Applications of this study include methods of incorporating gaseous fuels with very different characteristics into multi-fuel burners.

2. MATERIALS AND METHODS

The following experiments were conducted at the Reacting Flows and Turbulent Jets Laboratory at North Carolina State University in the Department of Mechanical and Aerospace Engineering. Fuels that were utilized were ethylene (CP Grade, 99.5% Pure) and methane (CP Grade, 99% Pure), while the diluents consisted of nitrogen and argon gases. The fuel nozzle measured 3.5-millimeters and was long enough to ensure that fully developed turbulent flow was present at the nozzle exit (length to diameter ratio much greater than ten). The volumetric flow rates of the fuel and inert gas were measured and regulated using an Advanced Specialty Gas Equipment Series 150 Flowmeter, and the images analyzed were taken using a Nikon D80 Digital SLR camera with an 18-105 millimeter Nikkor Lens.

Using the apparatus illustrated in Figure 2, each of the scenarios of fuel flow rate and inert gas dilution flow rate were examined. Utilizing each fuel separately with one of the two inert diluents being applied individually to the fuel, the liftoff heights of each of the flames were measured and an average liftoff height was determined from the ten measured liftoff heights for each case. The various scenarios consisted of varying the mole fraction at the nozzle exit of the inert diluent at levels of 0%, 5%, 10% and 20% by total mole fraction of the jet flow (the balance of the jet flow being the fuel of interest). Each average liftoff height was then plotted to determine the trend in comparison between stabilization heights of methane and ethylene and various levels of nitrogen and argon dilution. This experimental data is compared to theoretical predictions formulated by Broadwell et al. [24], and modifications to the scaling mechanisms in [24] are proposed for the cases examined.

3. THEORY

In studying a lifted flame, many theoretical studies have attempted to describe the phenomena that occur. An investigation was carried out by Yumlu [25] in 1968 for the laminar flame speed in these types of mixtures. Using Equation (1) given below, the "corrected" flame speeds were determined for both methane and ethylene, and for their corresponding mixtures percentages. The formulation given is

$$S_{u,m}^2 = (1-\alpha)S_{u,fuel}^2 \tag{1}$$

where $S_{u,m}$ is the burning speed of the mixture, α is the mass fraction of the inert diluent within the mixture, and $S_{u,fuel}$ represents the burning velocity of the pure fuel jet. However, by adding inert diluents to the fuel the temperature downstream is decreased. Thus, using the Arrhenius law, Equation (1) from Yumlu can be altered to

$$S_{u,m} = [1-\alpha]^{1/2} S_u^0 \exp\left(-\frac{E_a}{R}\left(\frac{1}{T_b}-\frac{1}{T_b^0}\right)\right) \tag{2}$$

where S_u^0 is the burning velocity of the pure fuel, Ea is the activation energy, R represents the universal gas constant, T_b is the mixture burning temperature (adiabatic temperature of the mixture), and T_b^0 is the burning temperature of the pure fuel (adiabatic temperature of the pure fuel jet) [25]. The laminar flame speeds for pure methane and ethylene jets are 0.39 m/s and 0.75 m/s, respectively [26].

Utilizing these equations, from Yumlu, the flame liftoff height dependence (x_l) for mixtures can be predicted using flame liftoff scaling given as

$$x_l \sim \left(u_0 d_0 \left(\frac{\rho_0}{\rho_\infty} \right)^{1/2} \left(\frac{\kappa}{S_{u,m}^2} \right) \right)^{1/2} \quad (3)$$

where u_0 is the local velocity, d_0 is the local diameter, ρ_0 is the pure fuel density, ρ_∞ is the surrounding air density, and κ is the thermal diffusivity [24]. This scaling is non-dimensionalized to determine the liftoff predictions for both fuels and the various scenarios of diluent levels. The non-dimensional formulation is given below in Equation (4).

$$x_{l,norm} = \frac{x_{l,y\%}}{x_{l,0\%}} \quad (4)$$

The notation of y% represents the various mole fraction percent levels used in each scenario. The variance in the equation compares a certain dilution level (numerator) to the control case of pure fuel jet (denominator). The non-dimensional scaling predictions of flame liftoff for the various scenarios of inert gas dilution are compared to the experimental findings presented in Figures 7 and 8.

4. RESULTS

Figures 3 and 4 give visual comparisons of varying fuels with various mole fraction dilution levels of inert gases. These visuals represent various incandescent trends as well as flame liftoff variances with nitrogen and argon diluents. Investigations of ethylene flames

produced similar results when diluting the pure fuel jet with various concentrations of nitrogen and argon. Figure 3(a) illustrates the pure ethylene flame in comparison to high levels of nitrogen dilution (20% by mole fraction), while Figure 3(b) gives the pure ethylene flame in comparison to high levels of argon dilution (20% by mole fraction). For both Figures 3(a) and 3(b) the fuel jet velocity is held constant at 49.73 m/s for the 0% dilution cases. However, the combined jet velocity is greater for the 20% dilution cases due to the addition of the inert gases. For the nitrogen-diluted case in Figure 3(a) the combined jet velocity at 20% dilution is 63.71 m/s, and for the argon-diluted case in Figure 3(b) the combined jet velocity at 20% dilution is 58.94 m/s. What should be noticed from these comparisons are the decreases in soot incandescence near the upstream portion of the reaction zone. The images illustrate that both nitrogen and argon dilution decrease the soot incandescence at the flame base at similar levels for high levels of dilution (20% by mole fraction). Both inert gases reduce the blackbody soot radiation that saturates the flame base, allowing the blue flame luminosity to become visible. Figures 4(a) and 4(b) give a similar comparison for methane jets; however, the pure methane flame is compared with 5% by mole fraction dilution cases for nitrogen and argon, respectively. A lower dilution level is shown due to the instabilities that are present with high dilution levels in methane flames (metastable flame liftoff and flame blowout/blowoff). It can be seen in Figures 4(a) and 4(b) that diluting methane flames has little effect on the flame luminosity. The varying flame radiance is visible due to low soot incandescence in both the near and far fields. This varies from the diluted ethylene flames in that only the near field soot incandescence is lowered due to the increase in inert gas dilution.

For ethylene, when both levels approach 20% by mole fraction, the flames experience similar levels of soot incandescence and flame luminosity for both diluents (Fig 3(a) and 3 (b)).

The methane comparison in Figures 4(a) and 4(b) show similar flame luminosity across the flame, as well as low soot incandescence. The rapid blowout/metastable phenomena that occurs with dilution levels above 5% mole fraction for methane is attributed to the smaller flammability limit of methane in comparison to that of ethylene flames, as well as, the higher flame speed of ethylene.

Initial results illustrate trends for fuel liftoff heights with increasing fuel velocity and inert diluent concentration. Each scenario of diluted methane and ethylene flames was plotted to observe various liftoff heights for changes in behavior at various dilution levels and fuel velocities. Figure 5 gives the plot of flame base heights (cm) from the fuel nozzle against the corresponding fuel velocity at the nozzle. This plot shows the liftoff heights for both nitrogen and argon dilution levels with methane. It should be noted that even small dilution mole fractions affect the liftoff of the flame drastically. The effect of nitrogen dilution on the lifted methane flame is much greater than that of the argon diluted scenario at lower levels of dilution, and argon proved to be more significant (that is, force the flame to liftoff higher) at higher levels of dilution. In comparison, ethylene jets were examined to have little disparity when comparing nitrogen and argon dilution levels. In comparing specific heats of nitrogen and argon, one finds that argon has a specific heat of ~0.52 KJ/(kgK), while nitrogen has a specific heat of ~1.04 KJ/(kgK). These variances in specific heat also attribute to the variances in liftoff in methane jets and not as much in ethylene jets due to the much higher adiabatic flame temperature of ethylene. An additional explanation behind this phenomenon is the much higher flame speed that exists with ethylene flames (approximately twice that of methane flames). This observation is addressed later when examining the theoretical scaling of the flame liftoff heights, while the observed trend is presented in Figure 6.

In comparison to Figure 5, with methane it can be seen that many fewer experimental points were determined due to the methane flame reaching blowout at much lower jet velocities than that of the ethylene flame. In addition, it can be seen that the ethylene flame requires a higher nozzle jet velocity to cause the flame to liftoff from the nozzle. To compare trends between different inert gases at the same levels of mole fraction dilution, the liftoff heights were non-dimensionalized and compared with the fuel mass flow rates. The mass flow rates are used to compare the non-dimensional heights due to the varying jet velocities between levels of diluent levels. By examining the mass flow rate of the fuel instead of the overall jet velocity, each of the levels of dilution fall in-line, with respect to the x-axis. Thus, it is easier to compare the non-dimensional liftoff heights across each level of dilution. Observing Figures 5 and 6 it can be seen that, unlike the methane liftoff progression, the ethylene data at the lower jet velocities is more compact and regardless of argon or nitrogen dilution levels the liftoff positions are closely related. Figures 7 and 8 give the non-dimensional liftoff heights for methane and ethylene, respectively. Referring to Figure 7, it can be seen that the non-dimensional trends for the methane data are similar. However, for the ethylene non-dimensional liftoff progressions in Figure 8 the values differ after 5% dilution levels of argon and nitrogen.

Referring to Figures 7 and 8, it can be seen for methane jets that the sensitivity of the flame is great when comparing the experimental non-dimensional liftoff heights to that of the non-dimensional flame liftoff scaling. In Figure 7, for methane, the 5% dilution levels of nitrogen and argon are similar in trend and non-dimensional value; however, when the dilution level is increased to 10% by mole fraction the points are separated. For ethylene, shown in Figure 8, the correlations are quite different. The experimental non-dimensional data suggests that the liftoff height for turbulent ethylene flames is less a function of inert diluent type, but

instead more dependent on the diluent mole fraction. This varies greatly from the data given from the methane, in that for turbulent methane jets the liftoff height is a function of *both* inert diluent type and diluent mole fraction. While diluting both methane and ethylene jets give similar variations in chemiluminescence with increasing levels of inert diluents regardless of diluent type, the liftoff progressions with increasing levels of diluents varies between the two fuels and the diluent being applied. Claiming that methane flame liftoff height is a function of both inert diluent and diluent mole fraction addresses the much lower flame speed of methane in comparison to ethylene. Thus, ethylene is not influenced as much by the diluents due to the speed/intensity at which the ethylene flame burns.

5. DISCUSSION

The observations regarding flame liftoff of methane and ethylene flames described validate the positions that methane flames are much more sensitive (that is, affected in a greater fashion) to dilution by inert gases than ethylene flames with the same/similar conditions. Observing the non-dimensional analysis of the experimental and theoretical results, it can be seen that a correlation constant might be introduced into Equation (4) to shift the theoretical data to approximately match the experimental results. This correlation constant is a ratio of the non-dimensional theoretical liftoff height to the non-dimensional experimental liftoff height.

Average values were determined for both methane and ethylene diluted jet flames. For the methane jets, the two inert diluents resulted in two correlation constants that vary greatly. This is due to the different effects that nitrogen and argon dilution have on methane jet flames. The average correlation constant for nitrogen diluted methane jets was determined to be 0.91, while the constant for argon diluted methane jets was determined to be 0.82. For ethylene jets the average correlation coefficients were very similar. This result defends the data illustrating that

the dilution of ethylene with nitrogen or argon will give similar liftoff heights for the same inert diluent mole fraction. The average correlation coefficient for nitrogen diluted ethylene jets was determined to be 0.79, while the constant for argon diluted ethylene jets was determined to be 0.77.

These correlations can be used with either nitrogen or argon diluted methane/ethylene turbulent jet flames. Therefore, the new non-dimensional formulation for the modified liftoff scaling is given below.

$$x_{l,norm,corrected} \cong \left(\frac{1}{C_H}\right) x_{l,norm} \tag{5}$$

This analysis of combining the two similar equations to determine the relationship with various levels of dilution is similar to that of Tieszan, et al. [28]. The method given by Tieszan et al., however, accounts for average turbulent jet flame speeds. The results presented exceed the limitation for Reynolds Number (>3,200) and, therefore, that formulation cannot be used [28]. Figures 9 and 10 give graphical comparisons of the experimental liftoff heights and the scaled non-dimensional liftoff prediction seen above in Equation (5) for both methane and ethylene, respectively [24]. The correlation constant for methane, in both diluent cases, has a greater effect on the experimental data, and thus forces the data to become more compact in Figure 9. For the ethylene plot, seen as Figure 10, it is established that the data undergoes minor modifications due to the more stable behavior of ethylene flames. This approximation method for non-dimensional flame liftoff height is valid over an average of liftoff heights that can be experimentally determined for various fuels. The correlation constant is related to the upper and lower flammability limits of the fuel being used. Thus, the higher the lower flammability limit and the lower the upper flammability limit for the fuel being considered, the more the correlation constant should fluctuate between diluents. This fluctuation is attributed to the sensitivity of the

pure fuel to the diluent being investigated. This sensitivity can be linked to the flammability limits of both methane and ethylene. Therefore, it can be concluded from the study given, that methane, is more sensitive to dilution than ethylene due to its much narrower flammability region, which leads to its correlation coefficient being much more unstable between fuels and higher in average value than that of ethylene. The physical significance of the non-dimensional correlation constant described is the relation to the flammability region, as well as the flame speed of the pure fuel being examined. The lower constant determined (for ethylene) assists in describing the fewer fluctuations that are present for ethylene jets. However, the larger constant determined for methane corresponds with the instabilities that are present in methane jets.

Further investigation should dilute methane and ethylene jet flames with other inert gases to determine if further correlation coefficients can be determined. The observation of the range of C_H could be tested as well for other fuels (such as propane) to determine if the coefficient indeed falls within the limits suggested. In addition to testing pure fuels with inert diluents, a further investigation should involve various fuel mixtures with inert diluents to determine fuel dominance in determining this correlation constant.

6. CONCLUSION

The various stabilization and blowout trends of methane and ethylene jet flames diluted with nitrogen and argon have been determined. Observing these methods and analyzing their significance in comparison to theoretical results, several conclusions can be made about the affects of dilution on methane and ethylene. The remarks addressing the sensitivity of the fuels to inert gases, stabilization patterns while diluted, influences on flame luminosity and soot incandescence, and non-dimensional trends with regards to flame liftoff heights are as follows:

1. Methane flame liftoff parameters are found to be much more sensitive to inert dilution than those of ethylene. This sensitivity is attributed to the flammability limit variation between the two fuels, as the lower flammability limit for methane is half of that of ethylene. Also, the upper flammability region for ethylene is nearly twice that methane. Thus, methane jets progress across the three stages of flame propagation (illustrated in Figure 1) much more rapidly than ethylene jets. In addition, these instabilities can be attributed to the much higher flame speed of ethylene in comparison to methane [26]. This conclusion has implications for utilizing biogases, as well as other low calorific gaseous fuels, in devices designed for methane combustion.
2. For ethylene flames, the liftoff height/flame behavior is less a function of the type of diluent being used, but, instead, a strong function of the mole fraction percentage being added to the fuel. However, this is not the case for methane flames. The methane flame liftoff height proved to be a function of both the diluent mole fraction percentage and the type of diluent added.
3. The luminosity of the two flames was greatly affected as the mole fraction percentage of the diluents increased. As diluent levels increased it was observed that the soot radiation was steadily decreased (especially near the flame base), and the level of blue flame luminosity appeared at the flame base with dilution, indicating the position of the flame leading edge.
4. Utilizing the flame liftoff scaling formulation to predict flame liftoff heights, the non-dimensional analysis performed demonstrated the greater sensitivity of methane to the diluents over ethylene. A correlation constant was incorporated into the non-dimensional flame liftoff analysis to determine if the trends are offset by certain scaling values. It was

determined that the two correlation constants for ethylene were relatively similar (which is due to the lack of dependence on diluent type for ethylene), while for methane the values varied. The results of integrating these correlation constants into the modified non-dimensional flame liftoff scaling resulted in the data from the non-dimensional calculations being shifted to closely match that of the non-dimensional measured values [24].

The findings presented in this paper shed light on the future of multi-fuel burner operation in that non-participatory species in the combustion process can have significant impacts on the flame anchoring/lifting process. This is of principal importance for adapting combustors for biogas/multi-fuel operation (burner geometry to produce stable reaction zone). Future investigations in progress involve examining other fuels and inert diluents (including CO_2, He, Ne) at similar mole fraction dilution levels, to observe if these trends can be broadly extended. Of particular interest is the independence of the ethylene flame behavior from inert diluent type, as well as how the guidelines for multi-fuel utilization in combustion systems will be impacted.

8. REFERENCES

[1] Schefer, R.W., 1994, "Stabilization of lifted turbulent jet flames," *Combust.* Flame, **99**, pp. 75-78.

[2] Terry, S.D. and Lyons, K.M., 2006, "Turbulent lifted flames in the hysteresis regime and the effects of coflow," *ASME J. Energy Resour. Technol.*, **128**(4), pp. 319-324.

[3] Gollahalli, S.R., Savas, Ö, Huang, R.F. and Azara, J.L.R., 1988, "Structure of attached and lifted gas jet flames in hysteresis region," *Proc. Combust. Instit.*, **21**(1), pp. 1463-1471.

[4] Iyogun, C.O. and Birouk, M., 2009, "Stability of a turbulent jet methane flame issuing from an asymmetrical nozzles with sudden expansion," *Combust. Sci. Technol.,* **181**(1), pp. 1443-1463.

[5] Pitts, W., 1988, "Assessment of theories for the behavior and blowout of lifted turbulent jet diffusion flames," *Proc. Combust. Instit.,* **22**(1), PP. 427-509.

[6] Lyons, K.M., 2007, "Toward an understanding of the stabilization mechanisms of lifted turbulent jet flames: experiments," *Prog. Energy Combust. Sci.,* **33**(2), pp. 211-231.

[7] Wilson, D.A. and Lyons, K.M., 2009, "On diluted-fuel combustion issues in burning biogas surrogates," *ASME J. Energy Resour. Technol.,* **131**(4), pp. 041802-041802-9.

[8] Stamps, D. and Tieszen, S., 2014, "Blowout of turbulent jet diffusion flames," *Fuel,* **118**, pp. 113-122.

[9] Moore, N.J., Terry, S.D. and Lyons, K.M., 2011, "Flame hysteresis effects in methane jet flames in air-coflow," *J. Energy Resour. Technol.,* **133**(2), pp. 319-324.

[10] Leung, T. and Wierzba, I., 2009, "The effect of co-flow stream velocity on turbulent non-premixed jet flame stability," *Proc. Combust. Instit.,* **32**(2), pp. 1671-1678.

[11] Cha, M.S. and Chung, S.H., 1996, "Characteristics of lifted flames in nonpremixed turbulent confined jets," *Proc. Combust. Instit.,* **26**, pp. 121-128.

[12] Moore, N.J. and Lyons, K.M., 2010, "Leading-edge flame fluctuations in lifted turbulent flames," *Combust. Sci. Technol.,* **182**(2), pp. 777-793.

[13] Moore, N.J., McCraw, J.L. and Lyons, K.M., 2008, "Observations on jet flame blowout," *Int. J. React. Syst.,* pp. 1-7.

[14] Takahashi, F., Mizomoto, M., Ikai, S. and Futaki, N., 1985, "Lifting mechanisms of free jet diffusion flames," *Proc. Combust. Instit.,* **20**(1), pp. 295-302.

[15] Wu, Y., Lu, Y., Al-Rahbi, I.S. and Kalghatgi, G.T., 2009, "Prediction of the lift-off, blow-out and blow-off stability limits of pure hydrogen and hydrocarbon mixture jet flames," *Int. J. Hydrog.* Energy, **34**, pp. 5940-5945.

[16] Moore, N.J., Kribs, J.D. and Lyons, K.M., 2011, "Investigation of jet-flame blowout with lean-limit considerations," *Flow Turbul. Combust.*, **87**(4), pp. 525-536.

[17] Karbasi, M. and Wierzba, I., 1998, "Prediction and validation of blowout limits of co-flowing jet diffusion flames—effect of dilution," *ASME J. Energy Resour. Technol.*, **120**(2), pp. 167-171.

[18] Chao, Y.C., Wu, C.Y., Lee, K.Y., Li, Y.H., Chen, R.H. and Cheng, T.S., 2004, "Effects of dilution on blowout limits of turbulent jet flames," *Combust. Sci. Technol.*, **176**, pp. 1735-1753.

[19] Wilson, D.A. and Lyons, K.M., 2008, "Effects of dilution and co-flow on the stability of lifted non-premixed biogas-like flames," *Fuel*, **87**(3), pp. 405-413.

[20] Choudhuri, A.R., Subramanya, M. and Gollahalli, S.R., 2008, "Flame extinction limits of H_2-CO fuel blends," *ASME J. Eng. Gas Turbines Power*, **130**(3), pp. 031501-1-031501-8.

[21] Kalghatgi, G.T., 1981, "Blow-out stability of gaseous jet diffusion flames," *Combust. Sci. Technol.*, **26**(5-6), pp. 233-239.

[22] Gollahalli, S.R., 1977, "Effects of diluents on the flame structure and radiation of propane jet flames in a concentric stream," *Combust. Sci. Technol.*, **15**(3-4), pp. 147-159.

[23] Smooke, M.D., McEnally, C.S., Fielding, J., Long, M.B., Pfefferie, L.D., Hall, R.J. and Colket, M.B., 2004, "Investigation of the transition from lightly sooting towards heavily sooting coflow ethylene diffusion flames," *Combust. Theory Model*, **8**, pp. 593-606.

[24] Broadwell, J.E., Dahm, W.J.A. and Mungal, M.G., 1984, "Blowout of turbulent diffusion flames," *Proc. Combust. Instit.,* **20**(1), pp. 303-310.

[25] Yumlu, V.S., 1968, "The effects of additives on the burning velocities of flames and their possible prediction by a mixing rule," *Combust. Flame,* **12**(1), pp. 14-18.

[26] Brown, C.D., Watson, K.A. and Lyons, K.M., 1999, "Studies on lifted jet flames in coflow: the stabilization mechanisms in the near- and far-fields," *Flow Turbul. Combust.,* **62**(3), pp. 249-273.

[27] Rajaratnam, N., 1976, "Turbulent Jets," Elsevier, New York, N.Y.

[28] Tieszan, S.R., Stamps, D.W. and O'Hern, T.J., 1996, "A heuristic model of turbulent mixing applied to blowout of turbulent jet diffusion flames," *Combust. Flame,* **106**(4), pp. 442-462.

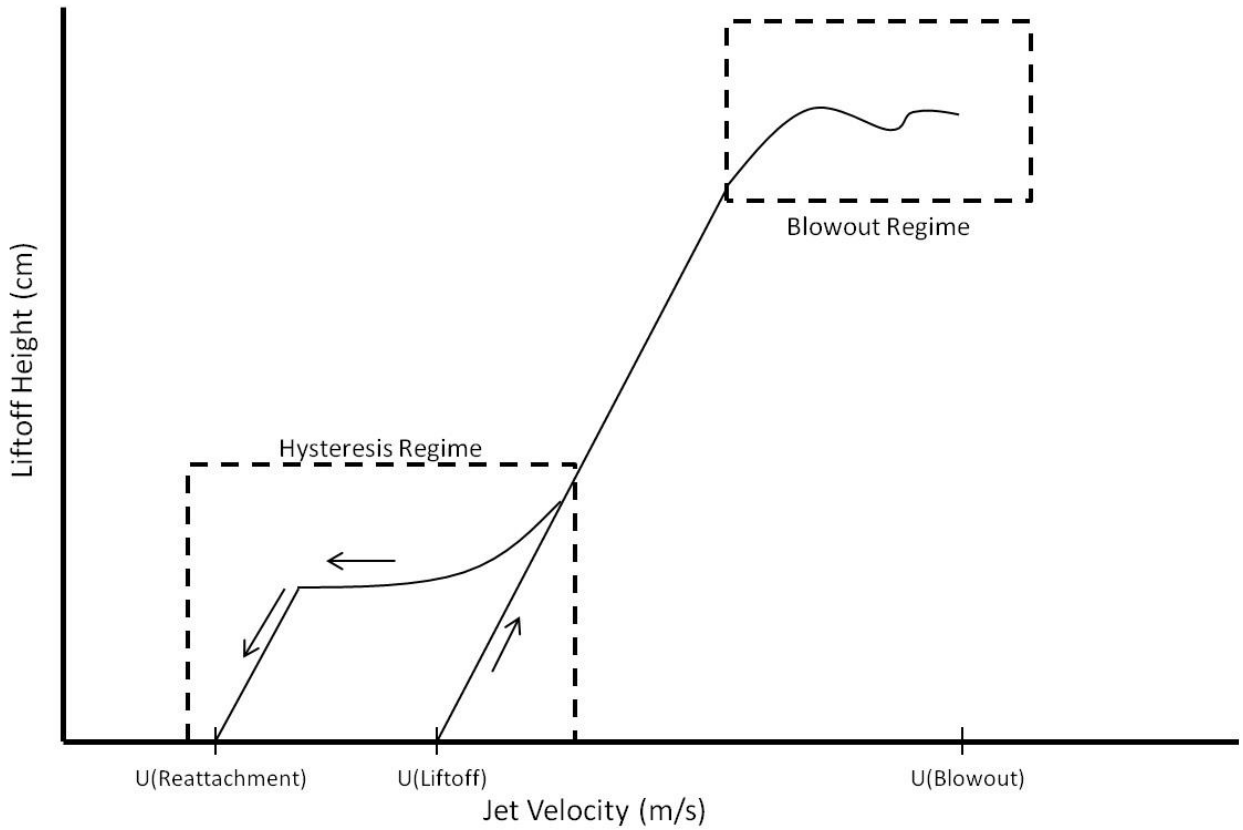

Figure 1: Flame stability plot demonstrating various phases in flame propagation

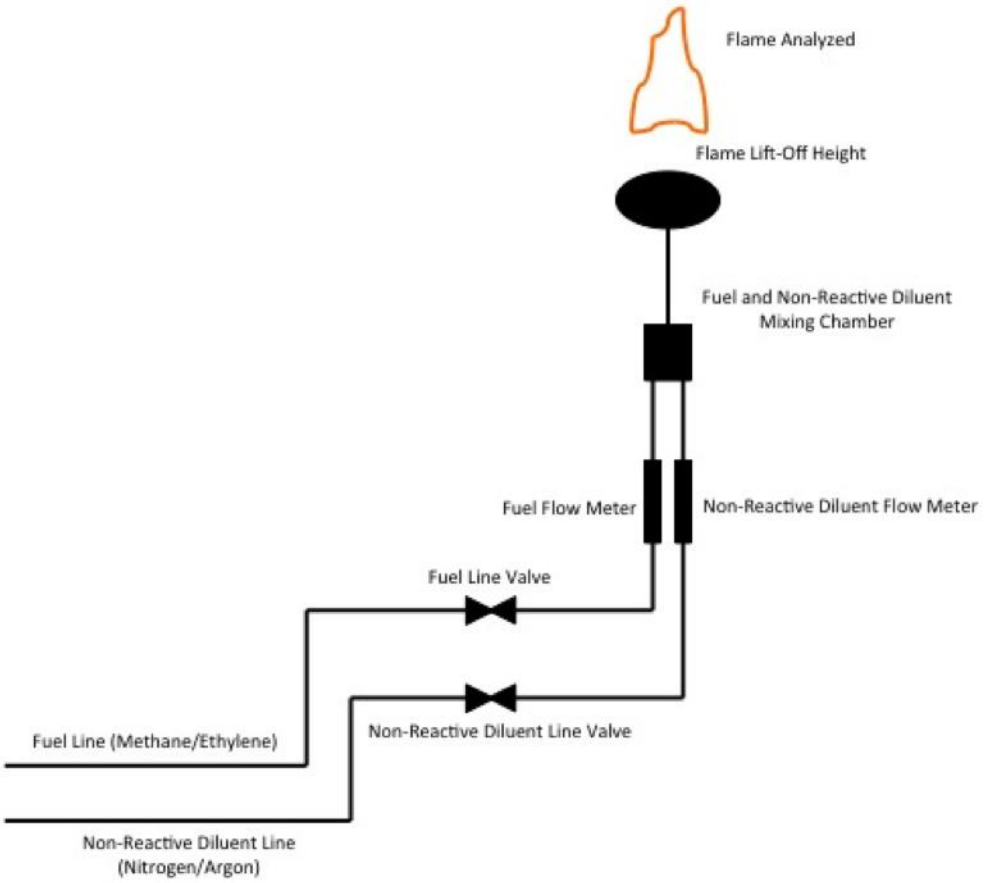

Figure 2: Apparatus schematic utilized for fuel (methane/ethylene) and non-reactive diluents (nitrogen/argon) mixing and combustion

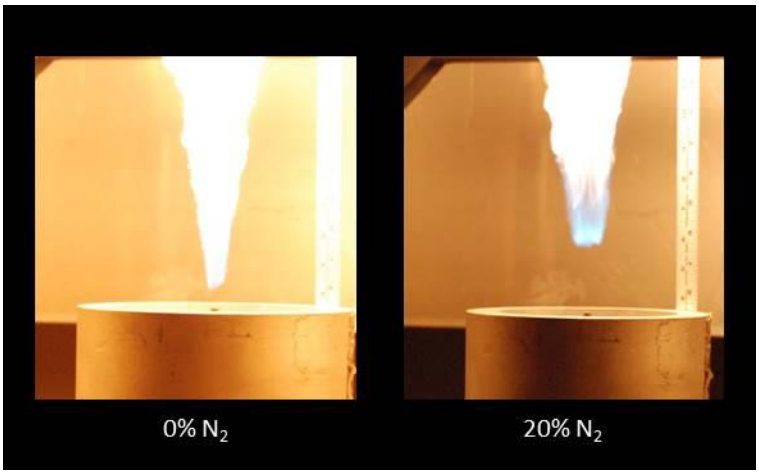

Figure 3(a): Pure ethylene flame luminosity in comparison to high level (20% by mole fraction) dilution of nitrogen.

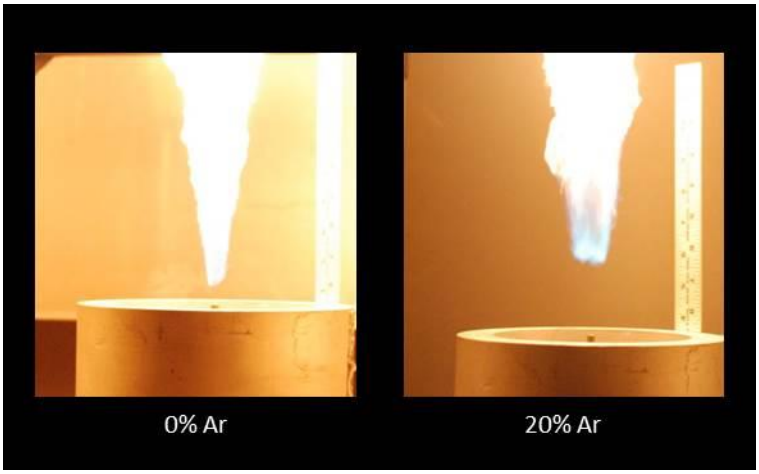

Figure 3(b): Pure ethylene flame luminosity in comparison to high level (20% by mole fraction) dilution of argon.

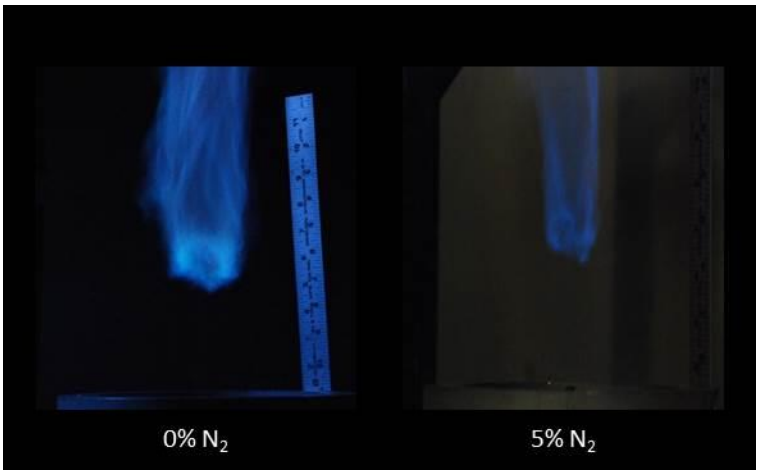

Figure 4(a): Pure methane flame luminosity in comparison to low level (5% by mole fraction) dilution of nitrogen.

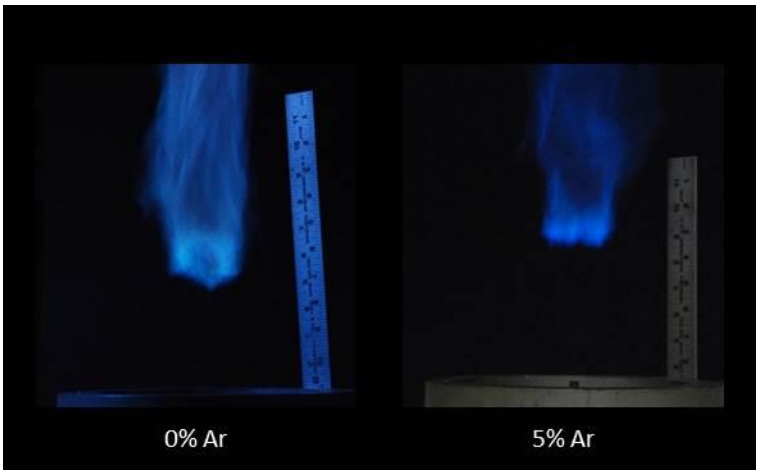

Figure 4(b): Pure methane flame luminosity in comparison to low level (5% by mole fraction) dilution of argon.

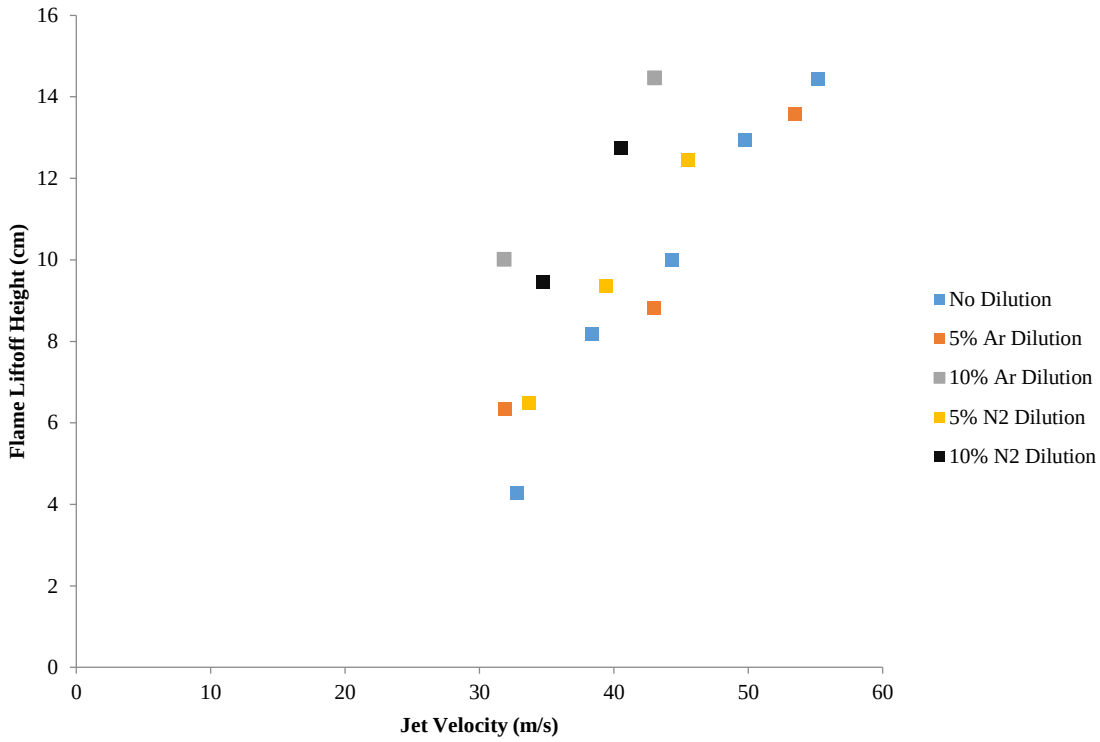

Figure 5: Trends of increasing methane jet flame liftoff height from the fuel nozzle with increasing fuel velocity and increasing inert gas dilution levels

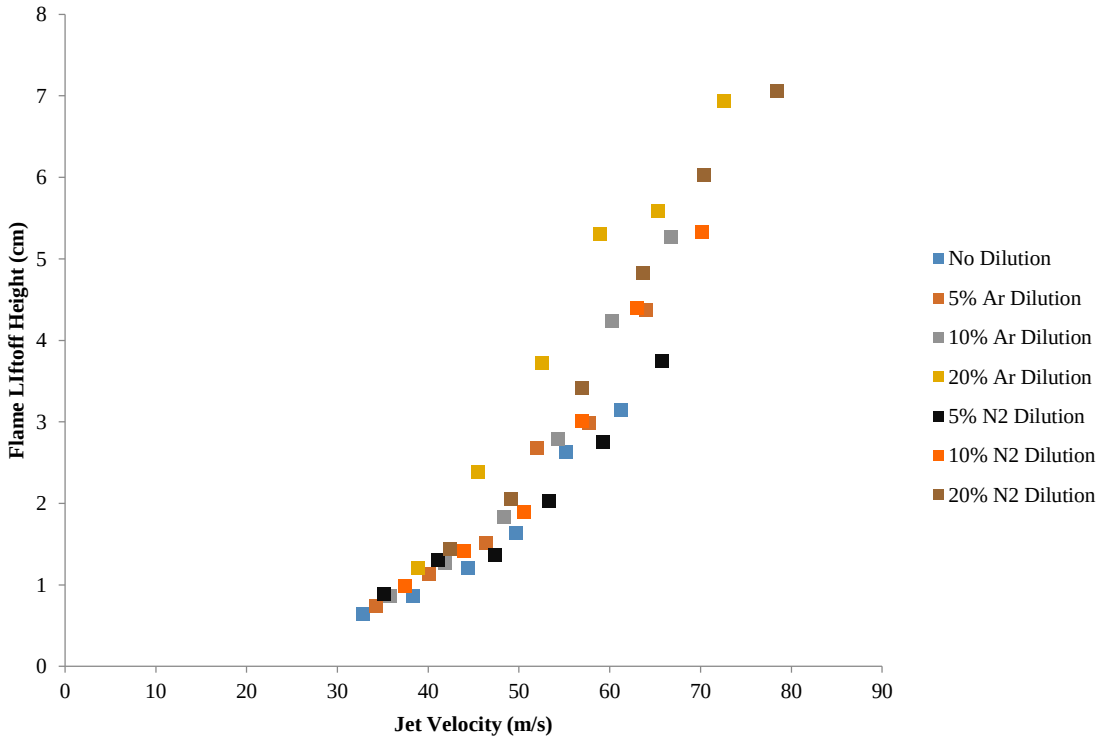

Figure 6: Trends of increasing ethylene jet flame liftoff height from the fuel nozzle with increasing fuel velocity and increasing inert gas dilution levels

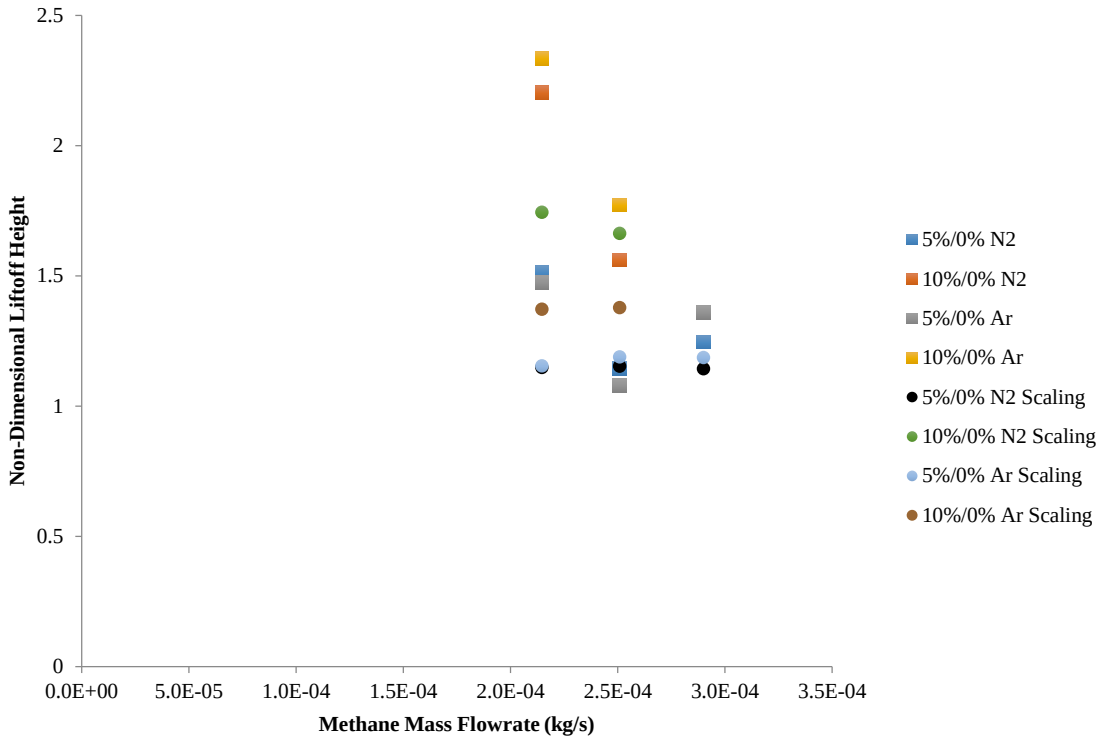

Figure 7: Trend of Non-Dimensional Methane Jet Flame Liftoff vs. Methane Mass Flowrate with comparison of experimental to theoretical non-dimensional liftoff height using the flame liftoff scaling formulation. The scaled points are those associated with the theoretical data, while the other points are experimental data points.

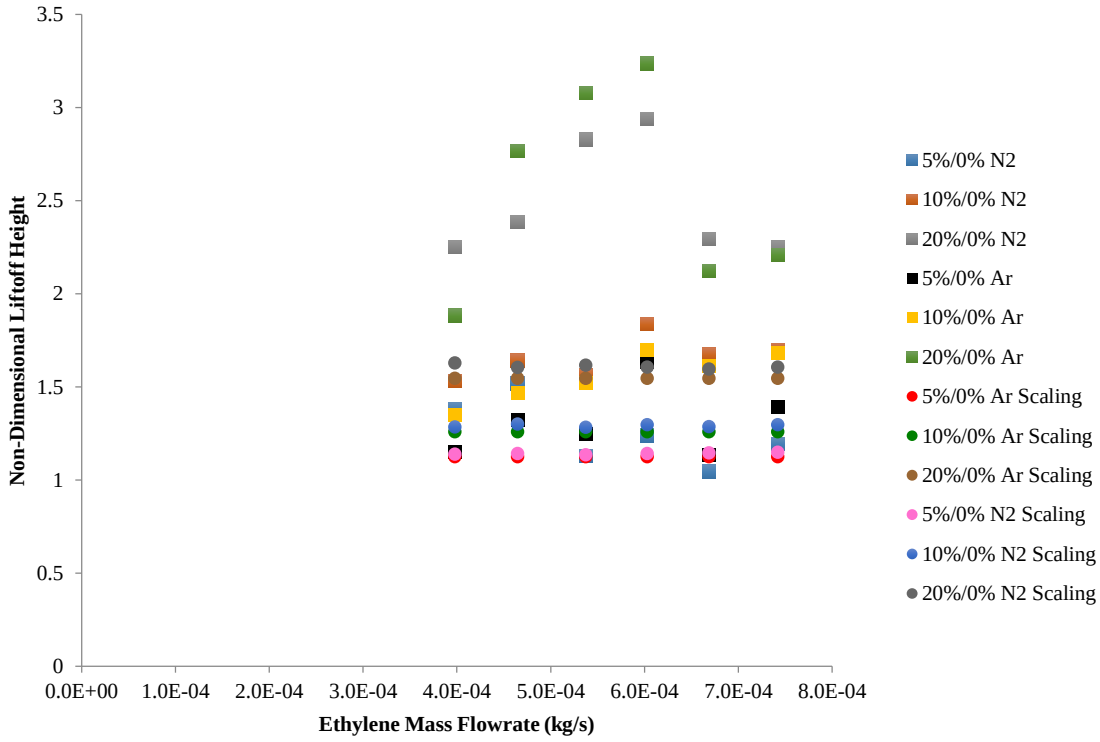

Figure 8: Trend of Non-Dimensional Ethylene Jet Flame Liftoff vs. Ethylene Mass Flowrate with comparison of experimental to theoretical non-dimensional liftoff height using the flame liftoff scaling formulation. The scaled points are those associated with the theoretical data, while the other points are experimental data points.

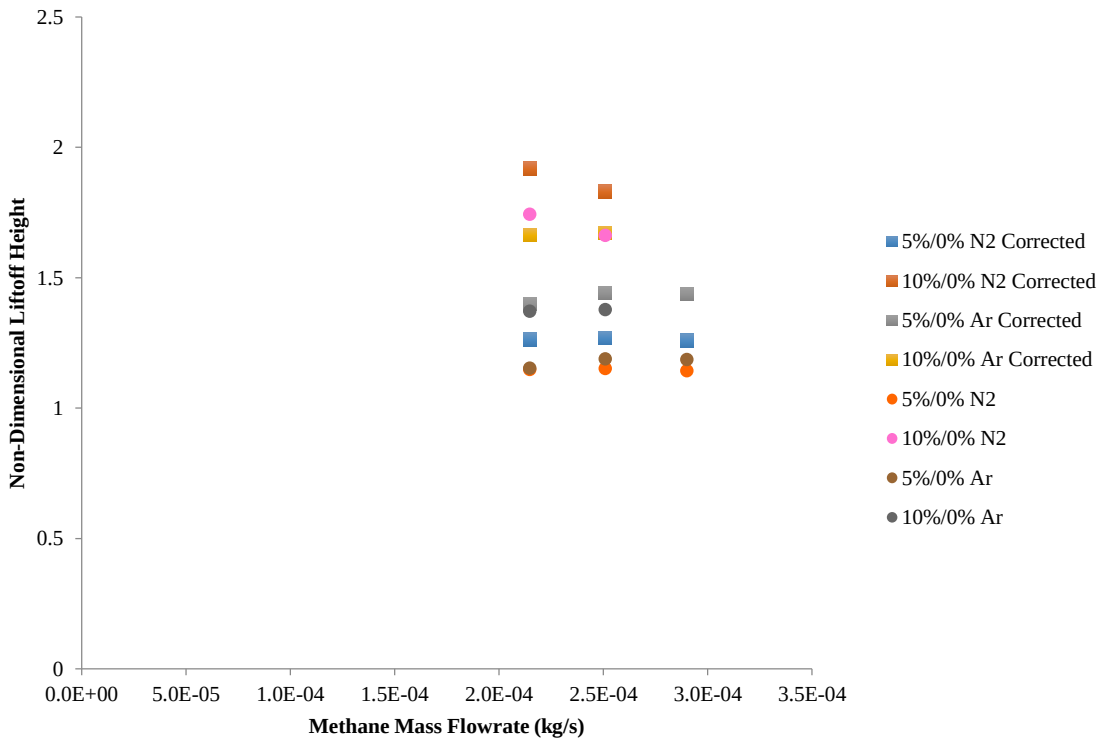

Figure 9: Comparison of Experimental Non-Dimensional Liftoff Heights To Corrected Theoretical Non-Dimensional Liftoff Heights using the non-dimensional modification to the flame liftoff scaling for methane jet flames. The corrected points are those associated with the theoretical data, while the other points are experimental data points.

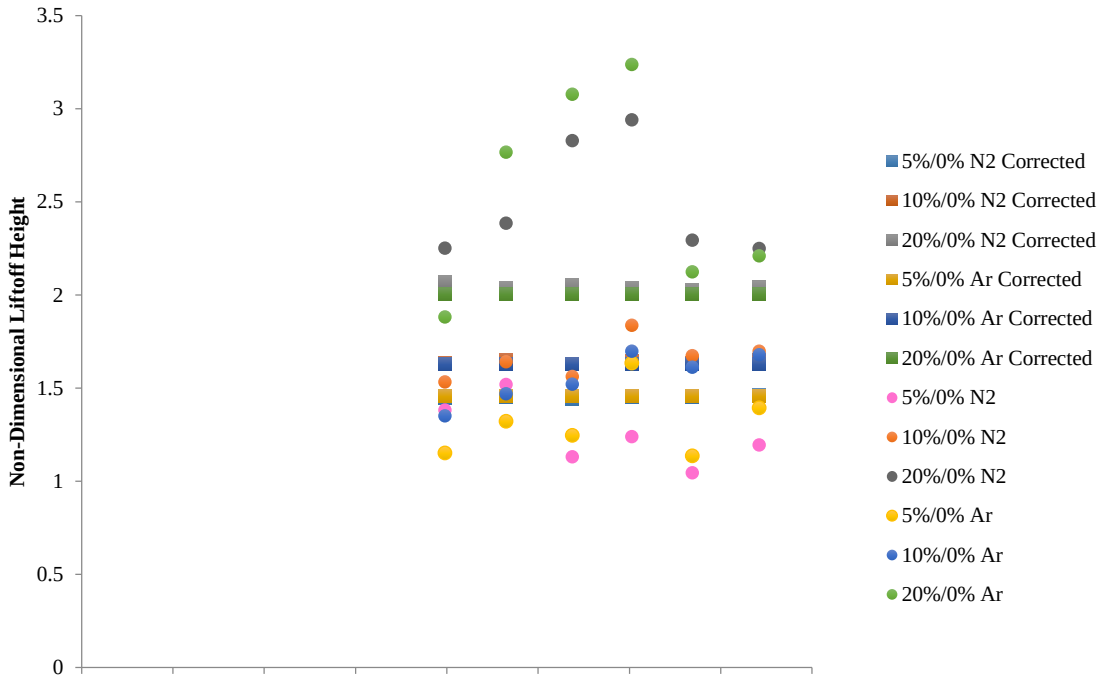

Figure 10: Comparison of Experimental Non-Dimensional Liftoff Heights To Corrected Theoretical Non-Dimensional Liftoff Heights using the non-dimensional modification to the flame liftoff scaling for ethylene jet flames. The corrected points are those associated with the theoretical data, while the other points are experimental data points.